AD-A032 490 SYRACUSE UNIV N Y F/G 9/5
RECTANGULAR FLAT-PACK LIDS UNDER EXTERNAL PRESSURE: IMPROVED FO--ETC(U)
SEP 76 C LIBOVE F30602-71-C-0312
UNCLASSIFIED RADC-TR-76-291 NL

1 OF 1
ADA032490

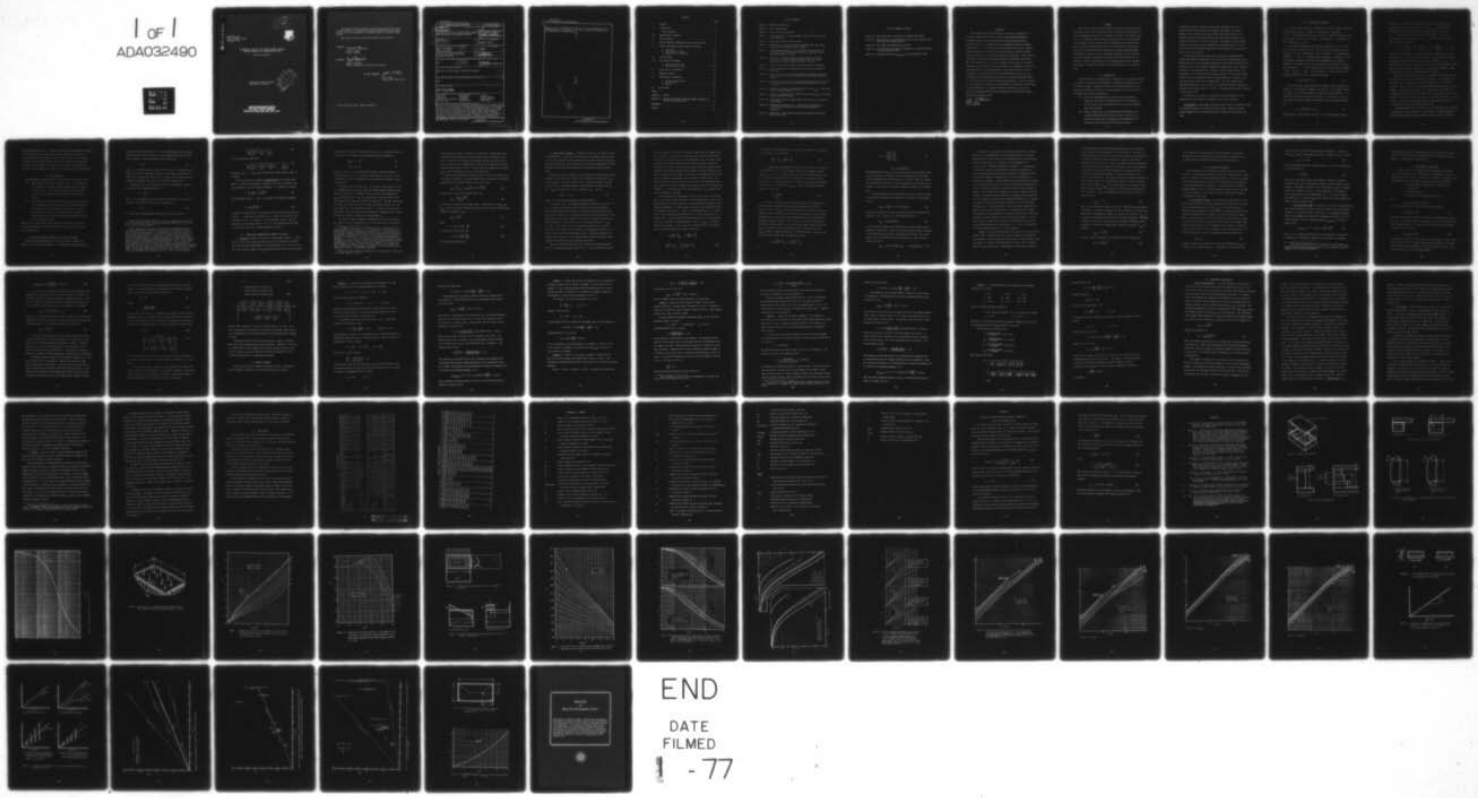

END

DATE
FILMED
1 -77

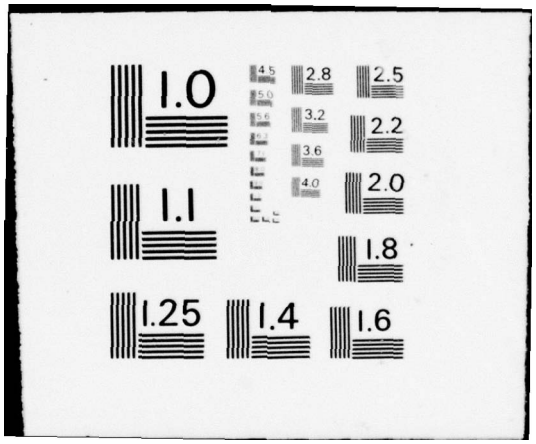
1.0
1.1
1.25
1.4
1.6
1.8
2.0
2.2
2.5
2.8
3.2
3.6
4.0
4.5
5.0
5.6

AD A032490

12 B.S.

RADC-TR-76-291
Final Technical Report
September 1976

# RECTANGULAR FLAT-PACK LIDS UNDER EXTERNAL PRESSURE: IMPROVED FORMULAS FOR SCREENING AND DESIGN

Syracuse University

Approved for public release;
distribution unlimited.

DDC
NOV 26 1976
C

ROME AIR DEVELOPMENT CENTER
AIR FORCE SYSTEMS COMMAND
GRIFFISS AIR FORCE BASE, NEW YORK 13441

This report has been reviewed by the RADC Information Office (OI) and is releasable to the National Technical Information Service (NTIS). At NTIS it will be releasable to the general public, including foreign nations.

This report has been reviewed and approved for publication.

APPROVED: Peter F. Manno

PETER F. MANNO
Project Engineer

APPROVED: Joseph J. Naresky

JOSEPH J. NARESKY
Chief, Reliability & Compatibility Division

FOR THE COMMANDER: John P. Huss

JOHN P. HUSS
Acting Chief, Plans Office

Do not return this copy. Retain or destroy.

UNCLASSIFIED

SECURITY CLASSIFICATION OF THIS PAGE (When Data Entered)

## REPORT DOCUMENTATION PAGE

READ INSTRUCTIONS BEFORE COMPLETING FORM

| | |
|---|---|
| 1. REPORT NUMBER: RADC-TR-76-291 | 2. GOVT ACCESSION NO. |
| 3. RECIPIENT'S CATALOG NUMBER | |
| 4. TITLE (and Subtitle): RECTANGULAR FLAT-PACK LIDS UNDER EXTERNAL PRESSURE: IMPROVED FORMULAS FOR SCREENING AND DESIGN. | 5. TYPE OF REPORT & PERIOD COVERED: Final Technical Report. June 1975 - June 1976. |
| | 6. PERFORMING ORG. REPORT NUMBER: N/A |
| 7. AUTHOR(s): Charles Libove | 8. CONTRACT OR GRANT NUMBER(s): F30602-71-C-0312 |
| 9. PERFORMING ORGANIZATION NAME AND ADDRESS: Syracuse University, 139 E. A. Link Hall, Syracuse NY 13210 | 10. PROGRAM ELEMENT, PROJECT, TASK AREA & WORK UNIT NUMBERS: 45400526 |
| 11. CONTROLLING OFFICE NAME AND ADDRESS: Rome Air Development Center (RBRM), Griffiss AFB NY 13441 | 12. REPORT DATE: September 1976 |
| | 13. NUMBER OF PAGES: 64 |
| 14. MONITORING AGENCY NAME & ADDRESS (if different from Controlling Office): Same | 15. SECURITY CLASS. (of this report): UNCLASSIFIED |
| | 15a. DECLASSIFICATION/DOWNGRADING SCHEDULE: N/A |

16. DISTRIBUTION STATEMENT (of this Report)

Approved for public release; distribution unlimited.

17. DISTRIBUTION STATEMENT (of the abstract entered in Block 20, if different from Report)

Same

18. SUPPLEMENTARY NOTES

RADC Project Engineer:
Peter F. Manno (RBRM)

19. KEY WORDS (Continue on reverse side if necessary and identify by block number)

| | | |
|---|---|---|
| Flat-packs | Bomb Pressure | Lid Seal |
| Hermeticity | Centrifuge | Tensile Stresses |
| Qualification Procedures | Reliability | Elastic Restraint |
| Screening Tests | Lid Deflection | Plate Theory |

20. ABSTRACT (Continue on reverse side if necessary and identify by block number)

Earlier work is improved and extended to provide formulas for the maximum tensile stress in the lid-to-wall seal, the maximum lid deflection, and the lid collapsing pressure for a rectangular flat pack under external pressure. It is shown how these formulas can facilitate (a) the proper design of the package so that it will retain its hermeticity and serviceability under a given screening pressure, and (b) the selection of a proper pressure to use in the hermeticity screening of an already designed package. Information is also given in the approximate equivalence of external pressure and centrifuge acceleration in

DD FORM 1 JAN 73 1473 EDITION OF 1 NOV 65 IS OBSOLETE

UNCLASSIFIED

SECURITY CLASSIFICATION OF THIS PAGE (When Data Entered)

339600 AB

regard to the seal stresses and lid behavior. Finally, experimental data on package hermeticity are presented, which tend to confirm the validity of the main hypotheses of the present work.

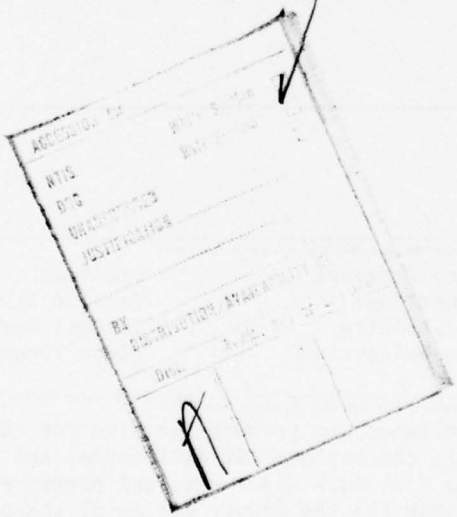

CONTENTS

LIST OF FIGURES

LIST OF FIGURES (continued)

## EVALUATION

This study was performed in support of the overall program of the Solid State Applications Section directed toward developing adequate reliability screening and qualification testing sequences for microelectronic devices in accordance with the Reliability Technical Program Objective No. 13. It successfully met its objective which was to provide a means for predicting the stress on the lid seal of a hermetic package under various levels of pressure and constant acceleration. These levels are included in the screening procedures imposed by MIL-M-38510 and MIL-STD-883. The results of the study will be used by the Air Force to establish effective test levels as a function of package size and material and also by part manufacturers as design guidelines. The equations which have been developed will be further verified by experimentation and then used for formulating revised screening requirements for proposed Test Method 5008, "Test Procedures for Hybrid and Multichip Microcircuits." This test method has been prepared for inclusion in MIL-STD 883A, "Test Methods and Procedures for Microelectronics" to complete the Center committment to the Joint Logistics Commanders Joint Technical Coordination Group Subtask on Hybrid Microcircuit Technology Base.

Peter F Manno

PETER F. MANNO
Project Engineer

## I. SUMMARY

Earlier work is improved and extended to provide formulas for the maximum tensile stress in the lid-to-wall seal, the maximum lid deflection, and the lid collapsing pressure for a rectangular flat-pack under external pressure. It is shown how these formulas can facilitate (a) the proper design of the package so that it will retain its hermeticity and serviceability under a given screening pressure, and (b) the selection of a proper pressure to use in the hermeticity screening of an already designed package. Information is also given on the approximate equivalence of external pressure and centrifuge acceleration in regard to the seal stresses and lid behavior. Finally, experimental data on package hermeticity are presented which tend to confirm the validity of the main hypotheses of the present work.

## II. INTRODUCTION

External pressure, per Method 1014.1 of Reference 1, is generally accepted as a means of screening out non-hermetic or potentially non-hermetic microelectronic packages. Knowing that this is the screening device to be employed, the designer and the user of such packages are faced then with the following two questions, respectively:

(a) Given the screening pressure to which the package will be subjected, what should the design features of the package be in order that a seal of good quality will retain its hermeticity under that pressure?

(b) Given a package that is already designed and available, what screening pressure should be used in order to weed out (i.e., destroy the hermeticity or aggravate the non-hermeticity of) those seals at the low end of the quality spectrum?

In Reference 2 simple formulas and charts were developed as an aid in answering these two questions for rectangular flat-packs. The work of Reference 2 was limited to the case in which the package walls were of constant thickness and material and the lid-to-wall seal extended across the entire thickness of the top of the wall. In Reference 3 this work was extended to include walls whose thickness and materials might vary from top to bottom and seals whose widths were narrow compared to the wall thickness at the top of the wall.

In the present paper we take these two questions up again and make further improvements and additions to the previous work (References 2 and 3). These include: (a) more reasonable definitions of the length and width of the package lid, (b) more reasonable assumptions regarding the elastic restraint furnished to the package walls by the base, (c) more complete data on lid deflections, (d) formulas for the ultimate strength of the lid under external pressure, and (e) experimental data on package hermeticity tending to validate the main hypotheses of the present work. Thus, the present report supersedes References 2 and 3, except for certain derivations in Reference 2 related to the present Figures 7, 8 and 11. These derivations are not repeated in the present work.

The symbols to be used are defined where first introduced, and the definitions are also compiled in Appendix A for ease of reference.

Acknowledgment.- This report was written under Contract No F30602-71-C-0312 for Advanced Reliability and Maintainability Studies with the Air Force System Command's Rome Air Development Center, Griffiss Air Force Base, New York.

## III. DESCRIPTION OF PACKAGES

The package configuration is rectangular, as shown in Figure 1, with the cavity having a width $a$, length $b$, and height $h$. Note that $a$ and $b$ are measured just under the lid and $a$ denotes the shorter of the two dimensions (if they are not equal). The dimension $h$ is assumed to be small compared to $a$ and $b$.

For analytical purposes the lid will be considered to be that part of the cover directly over the cavity. Thus the width and length of the lid are also $a$ and $b$, respectively. The lid thickness $t$ is assumed small compared to $a$ and $b$. The Young's modulus (modulus of elasticity) of the lid material is assumed to be known and is designated by the symbol $E$. Similarly, the Poisson's ratio of the lid material is assumed to be known and is denoted by $\nu$. For most materials there is little error in assuming $\nu = 0.3$. From $E$, $t$ and $\nu$ one can compute $D$, the so called "plate flexural stiffness" of the lid, defined as follows:

$$D \equiv Et^3/[12(1 - \nu^2)] \tag{1}$$

Two kinds of wall construction will be assumed, namely "uniform" and "stepped," as illustrated in Figures 2(a) and (b). In the former, which is typical of an all metal package, the material and the thickness $w$ are constant along the entire height of the wall. In this case $E_w$ and $\nu_w$ will denote the Young's modulus and Poisson's ratio of the wall material, and

$$D_w \equiv E_w w^3/[12(1 - \nu_w^2)] \tag{2}$$

will denote its plate flexural stiffness. In the stepped wall, which is

illustrated in Figure 2(b), the material and/or the thickness are only piece-wise constant. In such a wall $w$, $w_1$, $w_2$ ..., will denote the thicknesses of the several segments, starting from the top. $E_w$, $E_1$, $E_2$, ..., will denote their respective Young's moduli; $\nu_w$, $\nu_1$, $\nu_2$, ..., their Poisson's ratios; and $D_w$, $D_1$, $D_2$, ... their plate flexural stiffnesses, defined as follows:

$$D_w \equiv \frac{E_w w^3}{12(1-\nu_w^2)}, \quad D_1 \equiv \frac{E_1 w_1^3}{12(1-\nu_1^2)}, \quad D_2 \equiv \frac{E_2 w_2^3}{12(1-\nu_2^2)}, \quad \cdots \qquad (3)$$

The top of the top segment of the wall will have a height above the base that is equal to $h$, the depth of the cavity. The heights of the tops of the remaining segments above the base will be denoted by $h_1$, $h_2$, ..., respectively, as indicated in Figure 2(b). In a typical three-segmented stepped wall, like the one shown in Figure 2(b), the top segment might be a metal seal frame and the other two segments would be of glass.

Two kinds of lid-to-wall seal will be considered: the "wide seal" and the "narrow seal," which are illustrated in Figure 3. In the former, the seal width $w_s$ is essentially equal to the thickness $w$ of the top of the wall. This kind of seal would result typically from the use of a solder preform. In the narrow seal, which is the kind usually resulting from a cold-weld sealing process, the seal width $w_s$ is much smaller than $w$, and the seal is confined to the outer limits of the lid-wall interface. In such a seal, $e$ will denote the distance from the inner edge of the wall top to the middle of the seal width (see Figure 3(b)).

In the analytical work to follow it will be assumed that all four walls are identical, except possibly for their lengths. In actual packages the wall construction may be slightly different along one pair of parallel

sides than along the other. If that is the case, then for analytical purposes the construction of the longer sides sould be assumed to prevail on all four sides, unless the package is square or nearly square. If the package is square or nearly square separate calculations should be made assuming first one, then the other wall construction to prevail and the more conservative results adopted as the basis for any design or screening decisions.

## IV. MAIN HYPOTHESES

The following two hypotheses form the main basis of the present work:

(a) Under hydrostatic external pressure the lid of the package may be regarded as a uniformly loaded rectangular plate, of width $a$ and length $b$, with edges elastically restrained against rotation, this restraint being furnished by the walls of the package.

(b) The external pressure weeds out unsatisfactory seals by creating tensile stresses in the outer portions of the sealing material that exceed the tensile strength of that material. In poor quality seals (e.g., those containing voids or inclusions of foreign matter) this tensile strength will presumably be lower than in good quality seals.

Hypothesis (a) implies that we must determine the degree of elastic restraint furnished by the walls to the edges of the lid, and this is done in the next section.

## V. ELASTIC RESTRAINT FURNISHED TO THE LID BY THE WALLS

The walls will be regarded as wide vertical beams of length (i.e., height) $h$, with the local rotation $\theta$ (in radians) at the upper end pro-

portional to the local intensity $M$ of the bending moment per unit width exerted upon the wall by the lid as it flexes under under external hydrostatic pressure*. This relationship can be expressed as

$$M = k\theta \tag{4}$$

where $k$ is a proportionality constant. The value of $k$ depends upon the moment $M_b$ per unit width which the base of the package exerts upon the lower end of the wall (see Figure 4(a)). In what follows we will make the simplifying assumption that $M_b = M$, as shown in Figure 4(b).**

Assuming $M_b = M$, and analyzing the wall as a wide beam of length $h$, we arrive at the following formula for $k$:

$$k = \alpha \frac{D_w}{h} \tag{5}$$

where $\alpha$ is a dimensionless constant whose value depends on the nature of the wall. If the wall is uniform, as in Figure 2(a),

$$\alpha = 2 \tag{6a}$$

If the wall is a three-segmented stepped wall, as in Figure 2(b),

---

*The lid exerts a vertical force as well as a moment upon the inside edge of the top of the wall. The small additional bending of the wall due to this force is being neglected.

**This assumption is correct in the case of a uniform wall with the base and lid identical, for then a horizontal plane of symmetry exists at the mid-height of the package. It is also nearly correct in the case of short stubby walls (uniform or not) that effectively clamp the edges of the lid and base (which need not be identical). This is because the bending moments along the edges of a clamped rectangular plate under uniform pressure are virtually independent of the plate material and thickness, depending almost entirely on the pressure and the dimensions $a$ and $b$ (see Table 35 of Reference 4); thus the lid and base, having the same pressure and being about the same size, will have nearly identical distributions of bending moments around their edges when the latter are in a clamped or nearly clamped state. Since most packages fall fairly close to one or both of the two cases just described, the assumption $M_b = M$ is felt to be appropriate.

$$\alpha = \frac{2}{\frac{D_w}{h^2}\left(\frac{h^2-h_1^2}{D_w} + \frac{h_1^2-h_2^2}{D_1} + \frac{h_2^2}{D_2}\right)} \qquad (6b)$$

For an n-segmented stepped wall,

$$\alpha = \frac{2}{\frac{D_w}{h^2}\left(\frac{h^2-h_1^2}{D_w} + \frac{h_1^2-h_2^2}{D_1} + \frac{h_2^2-h_3^2}{D_2} + \ldots + \frac{h_{n-1}^2}{D_{n-1}}\right)} \qquad (6c)$$

Setting $D_1 = D_2 = \ldots = D_w$ in Eqs. (6b) and (6c) reduces them to (6a), as it should.

For later use we not introduce a dimensionless wall stiffness parameter, K, which is essentially a measure of the ratio of the wall flexural stiffness to the lid flexural stiffness. K is defined as follows:

$$K \equiv \frac{4}{\pi^2}\frac{k}{(D/a)} = \frac{4}{\pi^2}\frac{a}{h}\frac{D_w}{D}\alpha \qquad (7a)$$

If the Poisson's ratios $\nu$ and $\nu_w$ are equal, this definition reduces to

$$K = \frac{4}{\pi^2}\frac{a}{h}\frac{E_w}{E}\left(\frac{w}{t}\right)^3\alpha \qquad (7b)$$

In graphs to be given later, certain quantities are plotted as functions of arctan K, rather than as functions of K. Figure 5 will permit an easy conversion from K to arctan K. For most packages arctan K will be fairly close to the upper limit of $\pi/2$, or 1.57, implying that the edges of the lid are very close to being clamped by the walls.

## VI. FORMULA FOR MAXIMUM TENSILE STRESS IN THE SEAL

A. Derivation.- Under the action of a uniform gage pressure p (psi), reactions will develop along the edges of the lid, as depicted in Figure 6. These will include bending moments of varying intensity M (in.-lb per in.), due to the restraint against rotation furnished by the walls, and an effective

vertical shear of varying intensity V (lb per in.). The maximum values of M and V occur at the middle of the long side and can be expressed as

$$M_{max} = n_1 \cdot pa^2 \tag{8}$$

$$V_{max} = n_2 \cdot pa \tag{9}$$

where $n_1$ and $n_2$ are functions of the elastic restraint parameter K and the aspect ratio b/a of the lid. The values of $n_1$ and $n_2$ associated with any given configuration can be obtained from Figures 7 and 8, respectively.*

The maximum tensile stress $S_{max}$ in the seal is most likely to occur at the middle of the long side, where the bending moment transmitted from the lid to the wall is a maximum. At this location the bending moment $M_{max}$ and vertical shear $V_{max}$ are transferred to the edge strip of the cover directly over the wall, as shown in Figure 9.** The edge strip transfers these in turn to the top of the wall, along with the force pw per unit length due to the hydrostatic pressure P acting at the top of the edge strip. Thus, the edge strip is essentially a loading device to transfer the forces shown in Figure 9 to the wall below it.

The states of stress assumed to be developed at the top of the wall, as a result of the forces applied to it by the edge strip in the middle of

---

*In Figure 7 the data for a clamped plate ($K = \infty$, $\arctan K = \pi/2$) are taken from Table 35 of Reference 4. All other data in this figure are based on the analysis in Appendix A of Reference 2. In Figure 8 the data for a simply supported plate ($\arctan K = 0$) are from Table 8 of Reference 4. The data for a clamped plate ($\arctan K = \pi/2$) are based on the analysis in Appendix B of Reference 2. The curves for elastically restrained plates ($\arctan K = .4, .8., 1.2$) were inserted by interpolation, assuming a linear variation of $n_2$ with respect to $\arctan K$, which is approximately the variation obtained for $n_1$. In view of the small change in $n_2$ in going from simple support to clamping (around 6% at the most) and the small role that $n_2$ will play in the subsequent development, the linear interpolation employed in Figure 8 is considered acceptable.

**Recall that for analytical purposes we are considering the lid to end at the inner edges of the wall.

the long side, are shown in Figure 10. In the case of a wide seal we are assuming a linear variation of normal stress across the thickness of the wall. In the case of a narrow seal we assume instead a uniform tensile stress in the seal area together with a concentrated compressive line load along the inner edge of the wall. In both cases the maximum tensile stress $S_{max}$ in the seal material occurs at the outside edge.

The stress distributions of Figure 10 must be statically equivalent to the loading of Figure 9. For this equivalence one can deduce the following expressions for the maximum tensile stress in the seal:

$$S_{max} = \left( M_{max} + V_{max} \frac{w}{2} \right) \frac{6}{w^2} - \left( p + \frac{V_{max}}{w} \right) \tag{10a}$$

in the case of a wide seal (Figure 10(a)), and

$$S_{max} = \frac{M_{max} - \frac{1}{2} pw^2}{w_s e} \tag{10b}$$

in the case of a narrow seal (Figure 10(b)). Substituting for $M_{max}$ and $V_{max}$ their known values from Equations (8) and (9), we obtain the following formula for computing $S_{max}$:

$$S_{max} = p\left(\frac{a}{w}\right)^2 n \tag{11}$$

where

$$n = 6n_1 + 2n_2 \frac{w}{a} - \left(\frac{w}{a}\right)^2 \tag{12a}$$

in the case of a wide seal, and

$$n = \left[ n_1 - \frac{1}{2} \left(\frac{w}{a}\right)^2 \right] \frac{w^2}{e w_s} \tag{12b}$$

in the case of a narrow seal.

B. Application to Design.- Formulas (11) and (12) are the main results of the derivation. They can be of use both to the designer, whose objective is to design a package that will remain hermetic under a specified screening pressure, and the user, whose objective is to select an appropriate screening pressure that will destroy the hermeticity of packages with poor quality seals.

Considering first the designer, let us suppose that he knows the sealing material to be used and has a value for the allowable tensile stress $S_{all}$ of that material. Then his criterion for a satisfactory design, from the point of view of retaining hermeticity under external pressure, should be that $S_{max}$, as given by Eq. (12), be less than $S_{all}$. That is,

$$p \left(\frac{a}{w}\right)^2 n \leq S_{all} \tag{13}$$

where $p$ is the largest anticipated screening pressure.

In selecting $S_{all}$ the designer should of course be conservative. If $S_{all}$ is taken as the median tensile strength of the sealing material, then packages designed on the basis of the equality sign in Equation (13) will have a failure rate of approximately 50% even if properly sealed. (The failure rate will be still higher for a mixture of properly and improperly sealed packages.) On the other hand, if the designer selects for $S_{all}$ the lowest 1-percentile value of the material strength, then he should expect only a 1% failure rate for properly sealed packages designed on the basis of Equation (13) with the equality sign. The designer should also consider the possibility of the sealing material having a different tensile strength after deposition in the package than before.

There is one special precaution to be observed in applying Equation (13) to a stepped-wall package (Figure 2(b)). In such a package the upper-

most wall segment is typically a metal seal frame, while the segment below it is of glass. In that case, the critical seal could be the glass-metal interface (or the glass itself) at the underside of the seal frame, rather than the metal-to-metal bond at the top of the seal frame. This will certainly be the case if the latter bond forms a wide seal and the tensile strength of the sealing material there exceeds the tensile strength of the glass just below the seal frame. In any event, the designer should be sure that the inequality in Equation (13) is satisfied for both seals - the usually wide (but possibly narrow) one at the top of the seal frame, with $S_{all}$ based on the tensile strength of the sealant there; and the wide seal of width $w$ at the underside of the seal frame, with $S_{all}$ based on the tensile strength of the glass.

It could happen that the designer has very little data on the distribution of tensile strength values for the sealing material, or even on the mean strength, but he does know that a certain previously designed similar package, designated as I, when properly sealed with the same material had an acceptable failure rate $F$ under a screening pressure of $p_I$. Then in order for the new package, designated as II, to have a failure rate no greater than $F$ when properly sealed and subjected to its screening pressure $p_{II}$, he should so design package II that its $S_{max}$ is no greater than that of package I. Thus, referring to Equation (11), his criterion for a satisfactory design of package II should be

$$p_{II}\left[\left(\frac{a}{w}\right)^2 n\right]_{II} \leq p_I\left[\left(\frac{a}{w}\right)^2 n\right]_I$$

or

$$\left[\left(\frac{a}{w}\right)^2 n\right]_{II} \leq \frac{p_I}{p_{II}}\left[\left(\frac{a}{w}\right)^2 n\right]_I \qquad (14)$$

If the same screening pressure is to be used for package II as for package I, this design criterion becomes

$$\left[\left(\frac{a}{w}\right)^2 n\right]_{II} \leq \left[\left(\frac{a}{w}\right)^2 n\right]_{I} \tag{15}$$

C. Application to Screening.- Turning now to the user of an already designed package, let us first suppose that he has a minimum acceptable value, $S_{accept}$, for the tensile strength of the seal and wants to be sure of rejecting all packages with seal strengths less than that. Then he should select a screening pressure p such that the $S_{max}$ defined by Equation (11) is equal to or greater than $S_{accept}$. Thus, the required screening pressure is defined by

$$p \geq \frac{S_{accept}}{\left(\frac{a}{w}\right)^2 n} \tag{16}$$

It is more than likely, however, that the user of the package will not have enough information about the sealing material to be able to specify a value for $S_{accept}$, but he might know that in the past a certain pressure $p_I$ was considered suitable for the screening of a certain package, designated as I, employing the same sealing material as the present package, which we shall designate as II. Then his criterion for selecting a suitable screening pressure $p_{II}$ for the present package should be that the $S_{max}$ of package II, under the pressure $p_{II}$, be at least as big as the $S_{max}$ of package I under the pressure $p_I$. Referring again to Equation (11), we see that the criterion for selecting $p_{II}$ is then

$$p_{II}\left[\left(\frac{a}{w}\right)^2 n\right]_{II} \geq p_I\left[\left(\frac{a}{w}\right)^2 n\right]_{I}$$

or

$$p_{II} \geq p_I \frac{\left[\left(\frac{a}{w}\right)^2 n\right]_I}{\left[\left(\frac{a}{w}\right)^2 n\right]_{II}} \tag{17}$$

## VII. LID DEFLECTION

The maximum deflection $\delta_{max}$ of the lid under the lateral pressure p will occur at the center of the lid. Both the designer and the user must concern themselves with this deflection, in order to insure that during any screening the lid will not come in contact with the contents of the package. In this section we present formulas and graphs for estimating $\delta_{max}$.

An analysis based on the small-deflection theory of elastic plates is carried out in Appendix A of Reference 2 and leads to the following result:

$$\delta_{max} = n_4 \frac{pa^4}{D} = 12(1-\nu^2) \frac{p}{E} \left(\frac{a}{t}\right)^3 a n_4 \tag{18}$$

where $n_4$ is a function of K and b/a, whose value can be obtained from Figure 11. With $\nu$ taken as 0.3, this formula reduces to

$$\delta_{max} = 10.92 \frac{p}{E} \left(\frac{a}{t}\right)^3 a n_4 \tag{19}$$

It is well known, however, that small-deflection theory tends to overestimate the deflection. Figure 12 therefore presents curves from which a correction factor $n_5$, based on large-deflection theory, can be estimated. With this correction factor incorporated in them, the above formulas now read

$$\delta_{max} = 12(1-\nu^2) \frac{p}{E} \left(\frac{a}{t}\right)^3 a n_4 n_5 \simeq 10.92 \frac{p}{E} \left(\frac{a}{t}\right)^3 a n_4 n_5 \tag{20}$$

The graphs of $n_5$ (Figure 12) require some explanation. Although data for $n_4$ are available for K values ranging from 0 to $\infty$ (arctan K ranging from 0 to $\pi/2$), data for $n_5$ are available only for the limiting cases of simple support (K = arctan K = 0) and clamping (K = $\infty$, arctan K = $\pi/2$). Therefore interpolation between a K = $\infty$ graph and a K = 0 graph of Figure 12 may sometimes be needed in estimating $n_5$. A linear interpolation based on arctan K should be sufficiently accurate for practical purposes, although in most cases the assumption K = $\infty$ would also be suitable. A second difficulty associated with the estimation of $n_5$ derives from the fact that the large-deflection behavior of a plate is sensitive to whatever restraint the plate edges are under in regard to their movement in the plane of the plate. Graphs (a) and (c) of Figure 12 assume that such restraint is negligible; these graphs are felt to be appropriate when the wall stretching stiffness (e.g., $E_w hw$ in the case of a uniform wall) is small compared to the lid stretching stiffness, Eat. Graphs (b) and (c), on the other hand, assume that the edges are free to curve inward but not to strain along their length; these graphs are more appropriate for cases in which the wall stretching stiffness is large compared to the lid stretching stiffness. In most cases the use of Figure 12(c) alone will be sufficiently accurate for practical purposes and also conservative - i.e., it will over-estimate the lid central deflection due to a given pressure.

Figures 11 and 12 are both based on the premise of linear elasticity (Hooke's Law). Therefore they are, strictly speaking, not valid when the stresses in the lid become sufficiently high to initiate plastic flow (yielding). For lids of a brittle material, however, (e.g., ceramic) there is little plastic flow. Consequently, for such lids, deflection

calculations based on Equation (20) should be valid up to the point of fracture (which will be discussed in the next section). For lids of a ductile material, such as Kovar, there will be a plastic flow regime prior to complete collapse, in which deflections computed on the basis of Equation (20) will be too low. There is no general solution available for plate deflections in this regime, but fortunately there is some evidence to indicate that the plastic zones must be quite extensive before the elastic deflections become seriously in error (see Reference 7 and pp. 31-36 of Reference 6). One can infer from the discussion in Reference 6 that elastic theory may be sufficiently accurate as long as the maximum "effective stress" $\sigma_{e_{max}}$ in the lid, computed on the basis of elastic theory, does not exceed 1.5 $\sigma_y$, where $\sigma_y$ is the tensile yield stress of the lid material. Thus, an approximate criterion for the validity of Equation (20) is

$$\sigma_{e_{max}} < 1.5\ \sigma_y \tag{21}$$

where $\sigma_e$ is the effective stress of Von Mises' distortion-energy criterion of yielding. In order to facilitate the use of Equation (21), graphs from Reference 6 are presented in Figure 13, from which the values of $\sigma_{e_{max}}$ in the lid can be estimated for any value of the applied pressure. The graphs of Figure 13 are for the same four sets of boundary conditions as those of Figure 12. They give a dimensionless constant $n_6$ related to $\sigma_{e_{max}}$ as follows:

$$\sigma_{e_{max}} = n_6 E \left(\frac{t}{a}\right)^2 \tag{22}$$

In view of this relationship, the criterion (21) can be written as

$$n_6 < 1.5 \frac{\sigma_y}{E} \left(\frac{a}{t}\right)^2 \tag{23}$$

If this inequality is satisfied for any given pressure, a deflection calculation based on Equation (20) can be regarded as reliable; if not, one should assume that Equation (20) might be significantly low.

## VIII. LID COLLAPSING PRESSURE

Any calculation of seal stresses or lid deflection is, of course, not valid if the pressure exceeds that which will collapse the lid. Therefore it is important, in both screening and design, to be able to estimate the lid collapsing pressure, and in this section formulas are presented to facilitate making such an estimate. In presenting these formulas we consider separately lids of a brittle material, such as ceramic, and lids of a ductile material, such as Kovar, since the mechanism of collapse is different for both types.

A. Brittle-Material Lids.- For a structural element made of a perfectly brittle material it is often assumed that fracture will occur when the calculated maximum tensile stress $\sigma_{max}$ in the element equals the ultimate tensile strength $\sigma_t$ of the material. Ceramics employed for microelectronic packaging may not, however, be perfectly brittle in flexure. This is evidenced by the fact that quoted values of the modulus of rupture $\sigma_b$ (also called "flexural strength") of such ceramics are somewhat higher than the quoted values of $\sigma_t$ (see Reference 8 for examples). Therefore it may be more realistic for our purposes to take the following as a criterion of fracture or collapse of supposedly brittle-material lids:

$$\sigma_{max} \geq \sigma_b \tag{24}$$

In order to apply this criterion, one must have information on $\sigma_{max}$ as a function of the applied pressure p. Information of this kind is pre-

sented in Figure 14, which is based mainly on Reference 6. Figure 14 gives $\sigma_{max}$ through a dimensionless constant $n_7$ related to $\sigma_{max}$ as follows:

$$\sigma_{max} = n_7 E \left(\frac{t}{a}\right)^2 \tag{25}$$

This relationship permits the collapse criterion (24) for brittle-material lids to be written as

$$n_7 \geq \frac{\sigma_b}{E} \left(\frac{a}{t}\right)^2 \tag{26}$$

where $\sigma_b$ is a material constant (the modulus of rupture or "flexural strength") and $n_7$ can be estimated from Figure 14 for any given lid and pressure. The graphs of Figure 14 are for the same four sets of boundary conditions as Figures 12 and 13. In most cases part (c) of Figure 14 will be appropriate for the determination of $n_7$. For a more accurate determination of $n_7$, linear interpolation (based on arctan K) between the graphs of Figure 14 may be used.*

B. Ductile-Material Lids.- In the case of a plate of ductile material under lateral pressure, collapse is usually assumed to occur through the formation of plastic-hinge lines (yield lines). An approximate analysis based on that assumption is described in Appendix B and leads to the following expression for the collapsing pressure $p_{ultimate}$ of a ductile-material lid:

$$p_{ultimate} = \left[4 + 3.2 \frac{a}{b} + 3.5 \left(\frac{a}{b}\right)^2\right] \sigma_y \left(\frac{t}{a}\right)^2 \tag{27}$$

where $\sigma_y$ is the tensile yield stress of the lid material. Equation (27) is likely to be conservative, because in its derivation the possible

*Such linear interpolation is not rigorously correct, because $\sigma_{max}$ does not behave monotonically with arctan K, but small-deflection data suggests that it will be conservative.

strengthening effect due to membrane action was not taken into account. A graph of the bracketed term in Equation (27) can be found in Figure 22, where it is represented by the symbol $n_8$.

## IX. FLAT-PACKS IN A CENTRIFUGE

As part of the total screening process, packages are frequently spun in a centrifuge in such a way that the centrifugal force tends to push the lid into the cavity. As far as the lid alone is concerned, this centrifugal force is equivalent to a lateral pressure of Gtd, where

d = specific weight (weight per unit volume) of the lid material

t = thickness of lid

G = centripetal acceleration in units of g

and

g = acceleration of gravity.

If t is in inches and d in lbs per cubic inch, the formula

$$p_{equivalent} = Gtd \tag{27}$$

will give the effective pressure in psi due to a centrifuge acceleration of G g's. Alternatively, given any pressure p, we have from Equation (27) the following formula for the number of g's of centrifuge acceleration equivalent to that pressure:

$$G_{equivalent} = \frac{p}{td} \tag{28}$$

As an example of the use of this formula, let us consider a lid of .030 in. thickness and .302 $lb/in^3$ specific weight and ask how many g's of centrifuge acceleration are equivalent to a lateral pressure of 30 psi. From Equation (28) we obtain the following answer:

$$G_{equivalent} = \frac{30}{(.030)(.302)} = 3310 \text{ (g's)} \qquad (29)$$

By virtue of the equivalence relation (27), all the formulas and graphs of the preceding sections can be made to apply to a package in a centrifuge simply by replacing the symbol p everywhere by Gtd. In this way, for example, the following formula is obtained from Equation (20) for the central deflection of the lid of a package in a centrifuge:

$$\sigma_{max} = 10.92 \frac{Gtd}{E} \left(\frac{a}{t}\right)^3 a\, n_4\, n_5 \qquad (30)$$

where $n_5$ is to be obtained from the graphs of Figure 12 with the abscissa labels therein changed to $Gtda^4/Et^4$. Similarly, Equation (11) gives the following formula for the maximum tensile stress in the seal:

$$S_{max} = Gtd \left(\frac{a}{w}\right)^2 n \qquad (31)$$

It should be noted, however, that the interaction among the base, the walls, and the lid is slightly different for a package in a centrifuge than for the same package under hydrostatic pressure. Therefore the values of $\alpha$ to be used in Equations (7) for evaluating K are no longer strictly as given by Equations (6). The appropriate values of $\alpha$ depend on the manner in which the package is supported in the centrifuge.

Two possible types of support are illustrated in Figure 15. In the first, Figure 15 (a), the package is supported only along its edges. The lid and the base then deflect in the same direction (rather than in opposite directions, as they would under hydrostatic pressure). If the base and lid are identical the bending moment intensity $M_b$ acting upon the bottom of the wall will equal the bending moment intensity M acting

upon the top of the wall, and both bending moments will have the same sense. If the base and lid are not identical, the equality of $M_b$ and M does not hold; instead a reasonable assumption is

$$M_b = M\beta \tag{32}$$

where

$$\beta \equiv \frac{\text{mass of base}}{\text{mass of lid}} \tag{33}$$

and the base, like the lid, is considered to end where it meets the walls. Analyzing the wall as a wide beam under bending moments per unit width of M at the top and $M_b = M\beta$ at the bottom, both having the same sense, we arrive at the following formulas to replace (6a) and (6b), respectively.

$$\alpha = \frac{6}{2-\beta} \tag{34a}$$

$$\alpha = \frac{(6h^3/D_w)}{\left[ -3\beta h \left( \frac{h^2-h_1^2}{D_w} + \frac{h_1^2-h_2^2}{D_1} + \frac{h_2^2}{D_2} \right) + (2\beta+2)\left( \frac{h^3-h_1^3}{D_w} + \frac{h_1^3-h_2^3}{D_1} + \frac{h_2^3}{D_2} \right) \right]} \tag{34b}$$

The replacement for Equation (6c) can be written by noting the pattern of the terms in the denominator of Equation (34b) and extending it to n segments.

A more likely support condition is that illustrated in Figure 15(b). There the base is firmly bonded to a flat surface, producing an essentially clamped condition for the bottoms of the walls. The following formulas should then be used in place of (6a) and (6b), respectively:

$$\alpha = 4 \tag{35a}$$

$\alpha$ = Same expression as (34b), but with $\beta$ defined by Equation (36) below, instead of Equation (33). (35b)

$$\beta \equiv \frac{3h\left(\frac{h^2-h_1^2}{D_w} + \frac{h_1^2-h_2^2}{D_1} + \frac{h_2^2}{D_2}\right) - 2\left(\frac{h^3-h_1^3}{D_w} + \frac{h_1^3-h_2^3}{D_1} + \frac{h_2^3}{D_2}\right)}{\left[6h^2\left(\frac{h-h_1}{D_w} + \frac{h_1-h_2}{D_1} + \frac{h_2}{D_2}\right) - 6h\left(\frac{h^2-h_1^2}{D_w} + \frac{h_1^2-h_2^2}{D_1} + \frac{h_2^2}{D_2}\right) + 2\left(\frac{h^3-h_1^3}{D_w} + \frac{h_1^3-h_2^3}{D_1} + \frac{h_2^3}{D_2}\right)\right]} \tag{36}$$

Equation (35b) reduces to (35a), as it should, when $D_2 = D_1 = D_w$. To obtain a replacement for Equation (6c) we generalize Equations (35b) and (36) to an n-segmented wall by noting the pattern of each parenthetical grouping of terms.

Equations (34) and (35) will generally lead to larger $\alpha$'s (stiffer walls) than those obtaining under external pressure. Therefore, if the lid is already close to being clamped under external pressure (arctan K close to $\pi/2$), there is no need to bother with the above refinements in the $\alpha$ calculation when going to a centrifuge environment.

## X. NUMERICAL EXAMPLES

Here we pose and solve a.number of problems in order to demonstrate how the formulas and graphs of the preceding sections can be used.

Example 1.- A wide-seal uniform-wall Kovar package of the type shown in Figure 1 has the following dimensions (in inches):

$$a = b = .92 \quad t = .015 \quad h = .125 \quad w = .040$$

and the following material properties:

$$E = E_w = 20\times10^6 \text{ psi} \qquad \nu = \nu_w = .3 \qquad \sigma_y = 50 \text{ ksi}$$

We wish to find the maximum tensile stress in the seal and the central deflection of the lid due to an external screening pressure of 30 psi; also the pressure required to collapse the lid.

In accordance with Equation (6a) we take $\alpha$ to be 2, after which Equation (7b) and Figure 5 give

$$K = \frac{4}{\pi^2}\,\frac{.92}{.125}\left(\frac{.040}{.015}\right)^3 2 = 113 \qquad \arctan K = 1.56$$

(The closeness of arctan K to $\pi/2$ indicates that in effect the walls are clamping the edges of the lid.) Entering Figures 7, 8 and 11 with b/a = 1 and arctan K = 1.56, we obtain

$$n_1 = .051 \qquad n_2 = .443 \qquad n_4 = .00125$$

Also, for p = 30 psi, we have

$$\frac{pa^4}{Et^4} = \frac{30}{20\times10^6}\left(\frac{.92}{.015}\right)^4 = 21.1$$

Since the wall cross-sectional area (wh) is only around one-third of the lid cross-sectional area (ta) and arctan K is very close to $\pi/2$, we shall use parts (c) of Figures 12 and 13 to find

$$n_5 = .981 \qquad n_6 = 6$$

Equation (12a) then gives

$$n = 6(.051) + 2(.443)\left(\frac{.04}{.92}\right) - \left(\frac{.04}{.92}\right)^2 = .343$$

We now have all the constants needed to compute the quantities we are looking for. From Equation (11) we find the maximum tensile stress in the seal to be

$$S_{max} = 30\left(\frac{.92}{.04}\right)^2 (.343) \approx 5440 \text{ psi}$$

This would be a safe stress if the solder were one of the higher-strength types, such as a gold-tin alloy, but it could be only marginally safe if the solder were a lead-tin alloy. From Equation (20) we find the center deflection of the lid to be

$$\delta = 10.92\left(\frac{30}{20\times10^6}\right)\left(\frac{.92}{.015}\right)^3 (.92)(.00125)(.981) = .0043 \text{ in.}$$

which is only around 3 percent of the total depth of the cavity. To insure that the last calculation is not invalidated by plastic deformation, we shall check to see if the inequality (23) is satisfied. From the given data we have

$$1.5\,\frac{\sigma_y}{E}\left(\frac{a}{t}\right)^2 = 1.5\left(\frac{50\times10^3}{20\times10^6}\right)\left(\frac{.92}{.015}\right)^2 = 14.1$$

This exceeds $n_6$, which was found to be 6; therefore the inequality (23) is satisfied and the above computed deflection can be regarded as reliable. Finally, since Kovar is a ductile material, we shall use Equation (27) to find the lid collapsing pressure; it is

$$p_{ultimate} = (4 + 3.2 + 3.5)(50\times10^3)\left(\frac{.015}{.92}\right)^2 = 142 \text{ psi}$$

Thus, the given screening pressure of 30 psi is well below the value required to collapse the lid.

Example 2.- Suppose that 30 psi is considered to be a satisfactory screening pressure for the package of Example 1 (to be referred to as package I). What screening pressure would be appropriate for a second package (package II) identical in all respects to package I except for the dimension b, which has been increased to 1.92 in.?

For package II we still have arctan K = 1.56, but

$$\frac{b}{a} = \frac{1.92}{.92} = 2.1 \qquad \frac{a}{b} = .48$$

Figures 7 and 8 now give

$$n_1 = .083 \qquad n_2 = .513$$

and from Equation (12a) we obtain the following value of n for package II:

$$n = 6(.083) + 2(.513)\left(\frac{.04}{.92}\right) - \left(\frac{.04}{.92}\right)^2 = .541$$

Applying Equation (17), we find

$$p_{II} = (30)\left(\frac{.343}{.541}\right) = 19 \text{ psi}$$

to be an appropriate screening pressure for package II. That is to say, 19 psi applied to package II will produce the same $S_{max}$ in the seal as 30 psi applied to package I.

Example 3.- Return to the package of Example 1, assume that the seal is now of the narrow type (Figure 3(b)) with $w_s$ = .010 in., and determine the maximum tensile stress in the seal due to the 30 psi screening pressure.

With $w_s$ = .010 in., we have e = .035 in. Equation (12b) then gives

$$n = \left[.051 - \frac{1}{2}\left(\frac{.04}{.92}\right)^2\right] \frac{(.04)^2}{(.035)(.01)} = .229$$

From equation (11) we then find

$$S_{max} = 30\left(\frac{.92}{.04}\right)^2 (.229) = 3630 \text{ psi}$$

which is somewhat lower than that developed in the wide seal.

Example 4.- Assume that the package of Example 1 has its base changed from Kovar to ceramic with a thickness of .025 in., a modulus of elasticity of $50\times10^6$ psi, and a flexural strength of 65 ksi. What external pressure will cause the base to crack?

We shall imagine the package turned upside down, so that the base becomes in effect a lid with

$$t = .025 \text{ in.} \qquad E = 50\times10^6 \text{ psi} \qquad \sigma_b = 65 \text{ ksi}$$

and apply Equation (26). It gives

$$n_7 = \frac{65\times10^3}{50\times10^6}\left(\frac{.92}{.025}\right)^2 = 1.76$$

as the values of $n_7$ required to cause fracture. The extensional stiffness Eat of the ceramic base is much higher than the corresponding stiffness $E_w hw$ of the wall. Therefore parts (a) and (c) of Figure 14 are the ones that apply. Assuming that the walls essentially clamp the edges of the base* (as they do the lid), we narrow the choice further to part (c) alone. It gives the following as the value of $pa^4/Et^4$ needed to achieve an $n_7$ of 1.76 with a b/a of 1.0:

$$\frac{pa^4}{Et^4} = 5.6$$

whence the pressure required to crack the base is

*This assumption can be verified by determining K and noting that arctan K is still rather close to $\pi/2$.

$$p = \frac{5.6\ Et^4}{a^4} = \frac{5.6\ (50\times10^6)(.025)^4}{(.92)^4} = 153 \text{ psi}$$

This is slightly higher than the pressure of 142 psi that was found to be needed to collapse the lid (see Example 1).

Instead of assuming clamped edges (arctan K = $\pi/2$), we would have interpolated between Figures 14(a) and (c) on the basis of arctan K. However, Figure 14(a) alone give 6.1 as the required value of $n_7$. It is only 9% different from the value 5.6 furnished by Figure 14(c). Therefore interpolation is not warranted.*

Example 5.- Suppose the package of Example 4 to be placed in a centrifuge in such a way that the centrifugal force tends to push the ceramic base into the cavity. Taking the specific gravity of the ceramic to be 3.85, determine how many g's of centrifuge acceleration are required to crack the base.

We first convert the specific gravity of 3.85 to a specific weight, d, by multiplying it by the specific weight of water, which is .0361 lbs/in.$^3$. The result is

$$d = .139 \text{ lbs/in.}^3$$

The pressure required to crack the base is 153 psi, from Example 5. The equivalence relation (28) therefore gives

$$G = \frac{153 \text{ lb/in.}^2}{(.025 \text{ in.})(.139 \text{ lb/in.}^3)} = 44{,}000 \text{ g's}$$

of centrifuge acceleration required to crack the base. In this calculation, since the base is already close to being clamped at its edges, we have ignored the fact that of $\alpha$ may be different (higher) for centrifuge loading than for external pressure (see the discussion of this point in Section IX).

*A calculation using interpolation between Figures 14(a) and (c) has been carried out. It changes the computed base-cracking pressure by only 1 psi.

Equation (12a) then gives

$$n = 6(.051) + 2(.443)\left(\frac{.04}{.92}\right) - \left(\frac{.04}{.92}\right)^2 = .343$$

We now have all the constants needed to compute the quantities we are looking for. From Equation (11) we find the maximum tensile stress in the seal to be

$$S_{max} = 30\left(\frac{.92}{.04}\right)^2 (.343) = 5440 \text{ psi}$$

This would be a safe stress if the solder were one of the higher-strength types, such as a gold-tin alloy, but it could be only marginally safe if the solder were a lead-tin alloy. From Equation (20) we find the center deflection of the lid to be

$$\delta = 10.92\left(\frac{30}{20\times10^6}\right)\left(\frac{.92}{.015}\right)^3(.92)(.00125)(.981) = .0043 \text{ in.}$$

which is only around 3 percent of the total depth of the cavity. To insure that the last calculation is not invalidated by plastic deformation, we shall check to see if the inequality (23) is satisfied. From the given data we have

$$1.5\,\frac{\sigma_y}{E}\left(\frac{a}{t}\right)^2 = 1.5\left(\frac{50\times10^3}{20\times10^6}\right)\left(\frac{.92}{.015}\right)^2 = 14.1$$

This exceeds $n_6$, which was found to be 6; therefore the inequality (23) is satisfied and the above computed deflection can be regarded as reliable. Finally, since Kovar is a ductile material, we shall use Equation (27) to find the lid collapsing pressure; it is

$$p_{ultimate} = (4 + 3.2 + 3.5)(50\times10^3)\left(\frac{.015}{.92}\right)^2 = 142 \text{ psi}$$

Thus, the given screening pressure of 30 psi is well below the value required to collapse the lid.

Example 6.- A stepped-wall wide-seal package has the following dimensions (in inches):

$a = .365$ $\quad b = .670$ $\quad t = .025$

$h = .082$ $\quad h_1 = .060$ $\quad h_2 = .025$

$w = .040$ $\quad w_1 = .049$ $\quad w_2 = .071$

and the following mechanical properties:

$E = E_w = 20\times10^6$ psi (Kovar) $\quad E_1 = E_2 = 8.6\times10^6$ psi (glass)

$\nu = \nu_w = 0.3$ $\quad \nu_1 = \nu_2 = 0.2$

Determine the relationship between the pressure p applied to the lid and the maximum tensile stress $S_{max}$ produced in the seal.

From Equations (1) and (3) we have

$$D = \frac{(20\times10^6)(.025)^3}{12(.91)} = 28.6 \text{ in-lb}$$

$$D_w = \frac{(20\times10^6)(.040)^3}{12(.91)} = 117.5 \text{ in-lb}$$

$$D_1 = \frac{(8.6\times10^6)(.049)^3}{12(.96)} = 87.9 \text{ in-lb}$$

$$D_2 = \frac{(8.6\times10^6)(.071)^3}{12(.96)} = 267 \text{ in-lb}$$

Then Equation (6b) gives

$$\alpha = \frac{2}{1 - \left(\frac{h_1}{h}\right)^2 + \frac{D_w}{D_1}\left[\left(\frac{h_1}{h}\right)^2 - \left(\frac{h_2}{h}\right)^2\right] + \frac{D_w}{D_2}\left(\frac{h_2}{h}\right)^2}$$

$$= \frac{2}{1 - \left(\frac{.060}{.082}\right)^2 + \frac{117.5}{87.9}\left[\left(\frac{.060}{.082}\right)^2 - \left(\frac{.025}{.082}\right)^2\right] + \frac{117.5}{267}\left(\frac{.025}{.082}\right)^2}$$

$$= 1.82$$

whence (Equation (7))

$$K = \frac{4}{\pi^2} \frac{.365}{.082} \frac{117.5}{28.6} (1.82) = 11.1$$

Therefore (Figure 5)

$$\arctan K = 1.48$$

From the given dimensions we have

$$\frac{a}{b} = \frac{.365}{.670} = .545 \qquad \frac{b}{a} = 1.83$$

Entering these values, together with arctan K = 1.48, into Figures 7 and 8, we find

$$n_1 = .074 \qquad n_2 = .515$$

whence Equation (12a) gives

$$n = 6(.074) + 2(.515)\left(\frac{.040}{.365}\right) - \left(\frac{.040}{.365}\right)^2 = .542$$

Equation (11) then gives

$$S_{max} = p\left(\frac{.365}{.040}\right)^2 (.542) = 45.1\ p$$

Thus, for this package a factor of 45.1 applied to the pressure will give the maximum tensile stress in the seal. For example, a screening pressure of 100 psi will produce a maximum seal tensile stress of 4510 psi. Conversely, if one wishes to stress the seal to 5000 psi, a pressure of

$$p = \frac{5000}{45.1} = 111 \text{ psi}$$

is required.

## XI. EXPERIMENTAL CONFIRMATION

A. General Considerations.- Two main hypotheses form the basis of that portion of the present work dealing with hermeticity failure. The first is that the lid can be considered a uniformly loaded elastic rectangular plate with edges elastically restrained against rotation. It, together with certain assumptions regarding the distribution of stress across the width of the seal, leads to Equation (11) as the relationship between the external pressure p and the maximum tensile stress $S_{max}$ in the seal. The second main hypothesis is that loss of hermeticity occurs when $S_{max}$ reaches the ultimate tensile strength $S_{ult}$ of the seal material. This hypothesis, taken together with Equation (11), gives the following relationship between $S_{ult}$ and the critical pressure $p_{cr}$ required to cause loss of hermeticity:

$$S_{ult} = p_{cr}\left(\frac{a}{w}\right)^2 n$$

which can be rewritten as

$$p_{cr} = S_{ult}\left[\left(\frac{a}{w}\right)^2 n\right]^{-1} \tag{37}$$

Thus, the present hypotheses lead to a straight-line relationship between the pressure $p_{cr}$ causing loss of hermeticity and the package parameter $[(a/w)^2 n]^{-1}$, with the straight line passing through the origin and having a slope equal to the ultimate tensile strength $S_{ult}$ of the seal material (see Figure 16).

The validity of Equation (37), and therefore of the hypotheses on which it is based, can be tested by means of a fairly simple experimental program. The program would require flat-packs of various sizes and shapes, all carefully and uniformly sealed with the same material. With the aid of Equations (12) the value of $[(a/w)^2 n]^{-1}$ would be determined for each

package. Each package would also be subjected to an external pressure that is increased in small steps. The package would be leak-tested after each step, and the pressure $p_{cr}$ at which it first loses hermeticity would be noted. Thus, for each package a pair of coordinates would be obtained that could be plotted, using $[(a/w)^2 n]^{-1}$ as abscissa and $p_{cr}$ as ordinate. If the plotted points all fell on a single straight line through the origin, as in Figure 17(a), that would imply perfect validation of the theory (Equation (37)), and the slope of the line would give the effective ultimate tensile strength of the seal material.

Of course, such perfect agreement between theory and experiment is not to be expected, partly because of undoubted shortcomings in the theory and partly because of unavoidable variations in sealing quality among the packages. This variability in sealing quality produces, in effect, a spectrum of $S_{ult}$ values instead of a single one and would cause the test data to fall in a wedge-shaped band, as in Figure 17(b), with the angle of the wedge depending on the range of effective $S_{ult}$ values achieved in the seals. If the tests are performed using several groups of packages, with the packages nominally identical within each group but differing from group to group, the test data should fall as shown in Figure 17(c), provided that the range of variation of seal strengths was the same from group to group. If the range of seal strengths differed from group to group (as it might if the groups were of different size), the tops and bottoms of the vertical bars in Figure 17(c) would not lie on perfect straight lines through the origin. In that case, however, the <u>mean</u> $p_{cr}$ values of the various groups, being less sensitive to sample size than the <u>range</u> of $p_{cr}$ values, should still lie reasonably close to a single straight line. When the sample sizes in the various group are different, a <u>reduced range</u> of $p_{cr}$

values, covering one standard deviation above and below the mean $p_{cr}$ value, would be preferable to total range as a plotting parameter, because the standard deviation of the $S_{ult}$ values within any group of packages should also be less sensitive to sample size than the range of $S_{ult}$ values. A hypothetical plot of test data using such a reduced range is shown in Figure 17(d).

B. Test Program.- Data furnished to the author by a package manufacturer constitutes, in effect, a test program of the type described above. It involved 579 packages distributed among eighteen groups, with the packages nominally identical within each group. The packages had three-segment stepped-type walls, as in Figure 2(b). The top segment was a Kovar seal frame; the two lower segments were glass beads sandwiching a lead frame. The lids were Kovar and were sealed to the wall by means of a gold-tin solder preform.

Each group of packages was placed in a pressure bomb and subjected to external air pressure that was increased in small steps. Each new pressure was held for approximately 10 minutes, after which the packages were tested for gross leaks by submerging them in a heated liquid and watching for bubbles emanating from the interior of the package. The leakers were removed from the group and the rest of the group was then subjected to the next higher pressure.

The test program details are summarized in Table 1. Table 1 starts by giving the group designations (A1, A2, B, C, etc.) and the number of packages in each group. Lines 2 through 15 of the table then give the dimensional and material characteristics of the packages. It will be noted that groups A1 and A2 are nominally identical, as are groups G1 and G2. Thus, the results obtained from these two pairs of groups can serve to give

some indication as to the degree of inherent variability resulting from the manufacturing, assembly and testing procedures. Lines 16 through 24 represent stages in the calculations leading up to the value of the parameter $[(a/w)^2 n]^{-1}$ for each package group. Line 25 shows the pressure increment employed in the leak testing, and lines 26 to 30 give the main statistical information regarding the $p_{cr}$ values obtained for each group of packages. The detailed failure data on which lines 25 to 30 are based are contained in Table 2. In Table 2, p represents the pressure in psi and N the number of packages losing hermeticity at that pressure. Entries for which N = 0 are not included in the table.

C. Results.- Line 25 of Table 1 furnishes abscissa values for the types of plots discussed in Section A; ordinate values are obtained from one or more of the last five lines of Table 1.

The most significant representation of the results is that given in Figure 18, where the mean $p_{cr}$ values are plotted as a function of $[(a/w)^2 n]^{-1}$. Except for group P the mean $p_{cr}$ values fall reasonably close to a line emanating from the origin, as predicted by the theory. The solid straight line is the best fit, in a least-squares sense, to all the plotted points, excluding group P. Its slope leads to an inferred ultimate tensile strength of 8450 psi, which is considered quite reasonable for the glass beneath the seal frame.* Although there is some scatter of the test data relative to the straight line, it is not considered excessive in view of the inherent variability, as evidenced by the different mean $p_{cr}$ values for the nominally identical packages G1 and G2.

---

*The quoted strength of the gold-tin solder at the top of the seal frame is 18,900 psi. Therefore the glass, with quoted strengths of 10,200 psi and less, is considered to be the weak link in these packages.

The dashed straight lines in Figure 18 correspond to other inferred values for the tensile strength of the seal. It is seen that the stronger packages have an inferred seal strength of approximately 10,200 psi, which is one of the higher values quoted to the author for the tensile strength of the glass. The lowest dashed line shows that all of the packages achieved a mean inferred seal strength of 5000 psi or more. Packages P turned out to be considerably stronger, in terms of their mean $p_{cr}$ value, than the theory would indicate. There is no explanation for this discrepancy, although it may be significant that these packages are the most oblong, with a b/a ratio of 1.84. It is also interesting that the inferred seal strength for the P packages is 16,300 psi, which is not far from the 18,900 psi value quoted for the gold-tin solder preform. This agreement is undoubtedly coincidental, since the bubbles were observed to come from between the seal frame and the glass, not from between the seal frame and the lid.

In Figure 19, the test results are plotted in such a way as to show the range of $p_{cr}$ values from one standard deviation above the mean to one standard deviation below the mean. The fact that the heights of the bars tend to increase as the abscissa increases is considered a partial validation of the theory, since the theory predicts that a given range of seal strengths will lead to a range of $p_{cr}$ proportional to $[(a/w)^2 n]^{-1}$ (see Equation (37)).

In Figure 20, the entire experimental range of $p_{cr}$ values is plotted for each package. The heights of some of the vertical bars (e.g., in the case of the G1 packages) emphasize once again the degree of variability inherent in the $p_{cr}$ values of nominally identical packages and tend to support the author's earlier assertion that the scatter shown in Figure 18 is not excessive. The dashed lines in Figure 20 show that none of the individual packages had an inferred seal strength less than 3220 psi or greater than 18,000 psi.

In general the experimental results tend to confirm the theoretical hypotheses, although further investigation may be needed to explain the discrepancy between theory and experiment for the P group of packages.

## XII. CONCLUSIONS

Simple formulas have been presented that are related to the mechanical behavior of microelectronic flat-packs under external pressure and can assist in the design of such packages or the selection of suitable screening pressures for testing their hermeticity.

The specific items covered by the formulas are: maximum tensile stress in the lid-to-wall seal (or seal frame-to-glass bead seal), central deflection of the lid, pressure required to crack or collapse the lid, and the equivalence of external pressure and centrifuge acceleration insofar as lid behavior and seal stresses are concerned.

Numerical examples have been presented to illustrate the use of the formulas, and experimental data have been presented which tend to confirm the main hypotheses on which they are based.

From the numerical examples as well as the calculations related to the test specimens it appears that in most cases a simplifying assumption would be justifiable, namely the assumption that the edges of the lid are fully clamped by the walls to which they are joined. This permits one to set the elastic restraint parameter K equal to infinity ($\arctan K = \pi/2$), and thus avoid the sometimes tedious precise evaluation of this parameter.

TABLE 1.- TEST PROGRAM SUMMARY

| Group designation | | A1 | A2 | B | C | D | E | F | G1 | G2 | H | I | J | K | L | M | N | O | P |
|---|---|---|---|---|---|---|---|---|---|---|---|---|---|---|---|---|---|---|---|
| No. of packages in group | | 43 | 43 | 59 | 37 | 17 | 32 | 26 | 37 | 18 | 65 | 53 | 38 | 25 | 16 | 16 | 18 | 19 | 17 |
| Nominal dimensions (inches) | a | 1.129 | | .337 | .315 | .850 | .850 | .850 | .209 | | .209 | .772 | .774 | .788 | .545 | .547 | .650 | .630 | .365 |
| | b | 1.129 | | .337 | .315 | .910 | .910 | .910 | .332 | | .332 | .828 | .830 | .844 | .545 | .547 | .900 | .630 | .670 |
| | t | .030 | | .010 | .010 | .015 | .015 | .020 | .010 | | .010 | .030 | .030 | .030 | .015 | .015 | .015 | .015 | .025 |
| | h | .139 | | .054 | .048 | .083 | .117 | .117 | .050 | | .053 | .090 | .115 | .079 | .113 | .063 | .105 | .108 | .082 |
| | $h_1$ | .109 | | .044 | .038 | .068 | .087 | .087 | .042 | | .043 | .065 | .088 | .059 | .098 | .048 | .090 | .093 | .060 |
| | $h_2$ | .062 | | .027 | .018 | .045 | .060 | .060 | .020 | | .020 | .039 | .035 | .040 | .045 | .024 | .045 | .045 | .035 |
| | w | .0755 | | .023 | .030 | .045 | .046 | .046 | .0255 | | .0255 | .0515 | .0515 | .046 | .040 | .0365 | .0515 | .060 | .040 |
| | $w_1$ | .0825 | | .0285 | .0365 | .056 | .056 | .056 | .0295 | | .0295 | .059 | .059 | .0525 | .052 | .044 | .0655 | .069 | .049 |
| | $w_2$ | .1275 | | .0475 | .0675 | .088 | .0905 | .0905 | .064 | | .0475 | .092 | .089 | .0905 | .082 | .0715 | .098 | .110 | .071 |
| Material constants | E, $E_w$ | 20,000,000 psi | | | | | | | | | | | | | | | | | |
| | $E_1$, $E_2$ | 8,600,000 psi | | | | | | | | | | | | | | | | | |
| | $\nu$, $\nu_w$ | 0.3 | | | | | | | | | | | | | | | | | |
| | $\nu_1$, $\nu_2$ | 0.2 | | | | | | | | | | | | | | | | | |
| Derived quantities | b/a | 1 | | 1 | 1 | 1.07 | 1.07 | 1.07 | 1.59 | | 1.59 | 1.07 | 1.07 | 1.07 | 1 | 1 | 1.39 | 1 | 1.84 |
| | a/b | 1 | | 1 | 1 | .93 | .93 | .93 | .63 | | .63 | .93 | .93 | .93 | 1 | 1 | .72 | 1 | .54 |
| | $\alpha$ (Eq. 6b) | 1.58 | | 2.13 | 1.88 | 2.21 | 2.16 | 2.16 | 1.69 | | 1.65 | 1.82 | 1.58 | 1.96 | 2.09 | 1.86 | 2.02 | 1.61 | 1.82 |
| | K (Eq. 7a) | 82.7 | | 65.5 | 135 | 248 | 183 | 77.4 | 47.5 | | 43.7 | 31.9 | 21.9 | 28.5 | 77.6 | 94.2 | 206 | 243 | 13.5 |
| | arctan K | 1.556 | | 1.555 | 1.563 | 1.567 | 1.565 | 1.558 | 1.550 | | 1.548 | 1.539 | 1.525 | 1.536 | 1.558 | 1.560 | 1.566 | 1.567 | 1.497 |
| | $n_1$ (Fig. 7) | .050 | | .050 | .0505 | .0556 | .0556 | .0549 | .0756 | | .0755 | .0535 | .0526 | .0531 | .0501 | .0501 | .0715 | .0505 | .0755 |
| | $n_2$ (Fig. 8) | .443 | | .443 | .443 | .462 | .462 | .462 | .515 | | .515 | .461 | .461 | .462 | .443 | .443 | .508 | .443 | .516 |
| | n (Eq. 12a) | .355 | | .356 | .378 | .380 | .381 | .376 | .564 | | .564 | .378 | .373 | .369 | .360 | .355 | .503 | .378 | .554 |
| | $[(a/w)^2 n]^{-1}$ | .0126 | | .0131 | .0240 | .0074 | .0077 | .0078 | .0264 | | .0264 | .0118 | .0119 | .0092 | .0149 | .0125 | .0125 | .0240 | .0217 |
| Pressure increment (psi) | | 5 | 5 | 10 | 10 | 5 | 5 | 5 | 10 | 10 | 10 | 10 | 10 | 5 | 10 | 5 | 5 | 10 | 10 |
| $P_{cr}$ data (psi) | maximum | 110 | 110 | 180 | 250 | 55 | 55 | 50 | 400 | 300 | 240 | 140 | 150 | 90 | 180 | 115 | 120 | 220 | 390 |
| | minimum | 70 | 75 | 90 | 160 | 25 | 45 | 35 | 140 | 190 | 140 | 90 | 90 | 75 | 80 | 70 | 70 | 140 | 300 |
| | median | 90 | 110 | 140 | 190 | 45 | 50 | 42.5 | 270 | 240 | 200 | 120 | 120 | 85 | 120 | 105 | 100 | 190 | 360 |
| | mean | 92 | 97 | 139 | 202 | 45 | 51 | 43 | 273 | 247 | 192 | 121 | 123 | 84 | 124 | 92 | 98 | 183 | 353 |
| | std. dev. | 9.6 | 8.3 | 17.8 | 27.3 | 7.3 | 3.1 | 4.3 | 54.8 | 32.0 | 25.3 | 13.3 | 13.3 | 3.9 | 25.8 | 17.7 | 14.6 | 24.7 | 27.6 |



COPY AVAILABLE TO DDC DOES NOT PERMIT FULLY LEGIBLE PRODUCTION

TABLE 2.- LEAK TEST FAILURE DATA

| A1 | | A2 | | B | | C | | D | | E | | F | | G1 | | G2 | | H | | I | | J | | K | | L | | M | | N | | O | | P | |
|---|---|---|---|---|---|---|---|---|---|---|---|---|---|---|---|---|---|---|---|---|---|---|---|---|---|---|---|---|---|---|---|---|---|---|---|
| p | N | p | N | p | N | p | N | p | N | p | N | p | N | p | N | p | N | p | N | p | N | p | N | p | N | p | N | p | N | p | N | p | N | p | N |
| 70 | 1 | 75 | 2 | 90 | 1 | 160 | 1 | 25 | 1 | 45 | 3 | 35 | 2 | 140 | 1 | 190 | 1 | 140 | 3 | 90 | 1 | 90 | 1 | 75 | 1 | 80 | 1 | 70 | 4 | 70 | 1 | 140 | 2 | 300 | 1 |
| 75 | 1 | 80 | 1 | 110 | 4 | 170 | 8 | 35 | 1 | 50 | 18 | 40 | 11 | 150 | 1 | 200 | 1 | 150 | 7 | 100 | 6 | 100 | 1 | 80 | 8 | 90 | 1 | 75 | 2 | 75 | 2 | 150 | 1 | 310 | 1 |
| 80 | 5 | 85 | 3 | 120 | 9 | 180 | 4 | 40 | 2 | 55 | 11 | 45 | 9 | 160 | 1 | 210 | 1 | 160 | 2 | 100 | 9 | 110 | 3 | 85 | 12 | 100 | 1 | 80 | 1 | 85 | 1 | 160 | 1 | 320 | 1 |
| 85 | 7 | 90 | 3 | 130 | 7 | 190 | 7 | 45 | 7 | | | 50 | 4 | 230 | 3 | 220 | 1 | 170 | 2 | 120 | 16 | 120 | 18 | 90 | 4 | 110 | 2 | 105 | 7 | 90 | 1 | 170 | 4 | 330 | 2 |
| 90 | 10 | 95 | 10 | 140 | 20 | 200 | 1 | 50 | 4 | | | | | 240 | 4 | 230 | 2 | 180 | 3 | 130 | 11 | 130 | 10 | | | 120 | 4 | 110 | 1 | 95 | 3 | 180 | 1 | 340 | 2 |
| 95 | 7 | 100 | 13 | 150 | 10 | 220 | 3 | 55 | 2 | | | | | 250 | 4 | 240 | 5 | 190 | 9 | 140 | 10 | 140 | 4 | | | 130 | 3 | 115 | 1 | 100 | 2 | 190 | 3 | 360 | 2 |
| 100 | 5 | 105 | 9 | 160 | 3 | 230 | 10 | | | | | | | 260 | 3 | 260 | 2 | 200 | 18 | | | 150 | 1 | | | 140 | 2 | | | 105 | 5 | 200 | 2 | 370 | 5 |
| 105 | 4 | 110 | 2 | 170 | 3 | 240 | 2 | | | | | | | 270 | 2 | 280 | 2 | 210 | 11 | | | | | | | 170 | 1 | | | 115 | 1 | 210 | 4 | 380 | 1 |
| 110 | 3 | | | 180 | 2 | 250 | 1 | | | | | | | 280 | 1 | 290 | 2 | 220 | 4 | | | | | | | 180 | 1 | | | 120 | 2 | 220 | 1 | 390 | 2 |
| | | | | | | | | | | | | | | 290 | 5 | 300 | 1 | 230 | 4 | | | | | | | | | | | | | | | | |
| | | | | | | | | | | | | | | 300 | 2 | | | 240 | 4 | | | | | | | | | | | | | | | | |
| | | | | | | | | | | | | | | 310 | 2 | | | | | | | | | | | | | | | | | | | | |
| | | | | | | | | | | | | | | 320 | 4 | | | | | | | | | | | | | | | | | | | | |
| | | | | | | | | | | | | | | 330 | 1 | | | | | | | | | | | | | | | | | | | | |
| | | | | | | | | | | | | | | 340 | 1 | | | | | | | | | | | | | | | | | | | | |
| | | | | | | | | | | | | | | 380 | 1 | | | | | | | | | | | | | | | | | | | | |
| | | | | | | | | | | | | | | 400 | 1 | | | | | | | | | | | | | | | | | | | | |

## APPENDIX A: SYMBOLS

| | |
|---|---|
| $a$ | width of lid as measured inside the cavity, in. ($a \leq b$) |
| $b$ | length of lid as measured inside the cavity, in. ($b \geq a$) |
| $d$ | specific weight of lid material, lb/in.$^3$ |
| $D$ | plate flexural stiffness of lid, defined by Equation (1), in.-lb |
| $D_w$ | plate flexural stiffness of wall or of top segment of step-type wall, defined by Equation (2), in.-lb |
| $D_1$ | plate flexural stiffness of second segment of step-type wall, defined by Equation (3), in.-lb |
| $D_2$ | plate flexural stiffness of third segment of step-type wall, defined by Equation (3), in.-lb |
| $e$ | distance from inner edge of wall top to middle of width of narrow seal, in. |
| $E$ | Young's modulus of lid material, psi |
| $E_w$ | Young's modulus of wall or of top segment of step-type wall, psi |
| $E_1$ | Young's modulus of second segment of step-type wall, psi |
| $E_2$ | Young's modulus of third segment of step-type wall, psi |
| $g$ | acceleration of gravity, 32.2 ft/sec$^2$, 386 in/sec$^2$ |
| $G$ | centripetal acceleration in units of g, dimensionless |
| $G_{equivalent}$ | centripetal acceleration, in g's, equivalent to a given pressure, defined by Equation (28), dimensionless |
| $h$ | height of wall, measured inside cavity, in. |
| $h_1$ | height to top of second segment of step-type wall, in. |
| $h_2$ | height to top of third segment of step-type wall, in. |
| $k$ | wall rotational stiffness defined by Equation (4) and evaluated by Equation (5), in.-lb/in. |

| | |
|---|---|
| $K$ | dimensionless wall stiffness defined by Equations (7) |
| $m$ | fully plastic bending moment of lid, evaluated by Equation (B2), in.-lb/in. |
| $M$ | local bending moment per unit width at top of wall, in.-lb/in. |
| $M_{max}$ | maximum value of M, occurring at middle of long side, in.-lb/in. |
| $M_b$ | local bending moment per unit width at bottom of wall, in.-lb/in. |
| $n$ | number of segments in step-type wall, dimensionless |
| $n$ | dimensionless constant defined by Equation (11) and evaluated by Equations (12) |
| $n_1$ | dimensionless constant defined by Equation (8) and evaluated by Figure 7 |
| $n_2$ | dimensionless constant defined by Equation (9) and evaluated by Figure 8. |
| $n_4$ | dimensionless constant defined by Equations (18) and (19) and evaluated by Figure 11 |
| $n_5$ | large-deflection theory correction factor to $n_4$, defined by Equation (20) and evaluated by Figure 12, dimensionless |
| $n_6$ | dimensionless constant defined by Equation (22) and evaluated by Figure 13 |
| $n_7$ | dimensionless constant defined by Equation (25) and evaluated by Figure 14 |
| $n_8$ | dimensionless constant defined by Equation (B4), evaluated by Equations (B5) or (B6) or Figure 22. |
| $N$ | number of packages losing hermeticity at a given screening pressure, dimensionless |

| | |
|---|---|
| $p$ | net pressure acting inward on lid, psi |
| $p_{cr}$ | pressure causing loss of hermeticity, psi |
| $p_I$ | screening pressure for a previous package, psi |
| $p_{II}$ | screening pressure for a new package, psi |
| $p_{equivalent}$ | effective pressure due to a centrifuge acceleration, defined by Equation (27), psi |
| $p_{ultimate}$ | collapsing pressure for ductile-material lid, psi |
| $S_{accept}$ | minimum acceptable strength of seal material, psi |
| $S_{all}$ | allowable tensile stress in seal, psi |
| $S_{max}$ | maximum tensile stress in seal, psi |
| $t$ | thickness of lid, in. |
| $V$ | effective vertical shear intensity at edge of lid, lb/in. |
| $V_{max}$ | maximum value of V, occurring at middle of long side, lb/in. |
| $w$ | thickness of wall or of top segment of wall, in. |
| $w_1$ | thickness of second segment of step-type wall, in. |
| $w_2$ | thickness of third segment of step-type wall, in. |
| $w_s$ | width of seal, in. |

GREEK:

| | |
|---|---|
| $\alpha$ | dimensionless proportionality constant defined by Equation (5) and evaluated by Equations (6), (34) or (35) |
| $\beta$ | constant defined by Equation (32) and evaluated by Equations (33) or (36) |
| $\delta_{max}$ | central deflection of lid, in. |
| $\theta$ | local angle of rotation of top of wall, radians |
| $\mu$ | parameter defined in Figure 21, dimensionless |
| $\nu$ | Poisson's ratio of lid material, dimensionless |
| $\nu_w$ | Poisson's ratio of wall or of top segment of step-type wall, dimensionless |

| | |
|---|---|
| $\nu_1$ | Poisson's ratio of second segment of step-type wall, dimensionless |
| $\sigma_b$ | flexural strength (bending modulus of rupture) of lid material, psi |
| $\sigma_{max}$ | maximum tensile stress in lid, psi |
| $\sigma_{e_{max}}$ | maximum effective stress in lid, psi |
| $\sigma_t$ | ultimate tensile strength of lid material, psi |
| $\sigma_y$ | tensile yield stress of lid material, psi |

## APPENDIX B:

## ORIGIN OF COLLAPSING PRESSURE FORMULA, EQUATION 27, FOR DUCTILE-MATERIAL LIDS

The uniform lateral pressure required to collapse a plate of ductile material can be estimated by means of a "yield-line analysis" similar to the limit analysis technique used for rigid-jointed frames. The yield-line analysis method is explained in Reference 9.

Applying this method to the rectangular lid of a flat pack, with an assumed yield-line pattern as represented by the dashed lines in Figure 21, and with $\mu$ therein so chosen as to minimize the collapse load, one easily arrives at the following formula for the collapsing pressure, $p_{ultimate}$, for the case $a/b \leq 1$:

$$p_{ultimate} = \frac{48}{\left[\sqrt{3 + (a/b)^2} - (a/b)\right]^2} \frac{m}{a^2} \qquad (B1)$$

where m is the "fully plastic bending moment" per unit length of yield line, acting across the yield lines. For a non-strain-hardening material with the same yield stress $\sigma_y$ in tension and compression,

$$m = \sigma_y \, t^2/4 \qquad (B2)$$

and we shall assume the same relationship to apply, as an approximation, to a strain-hardening material, taking $\sigma_y$ in that case to be the 0.2% offset yield stress.

The yield-line pattern of Figure 21 is a plausible one for the limiting case $a/b \to 0$. However, at the other limit, $a/b = 1$, E. N. Fox (Reference 10) has found that a more sophisticated yield line arrangement prevails which leads to a collapsing pressure of $42.8\ m/a^2$ in place of

the value of 48 $m/a^2$ given by Equation (B1). Thus it appears that Equation (B1) requires a correction factor of 42.8/48 at a/b = 1 and a correction factor of 1 at a/b = 0. For simplicity, we shall assume the correction factor to vary linearly with respect to a/b between these two end points, thus to have the form

$$1 - \frac{5.2}{48}\frac{a}{b} \tag{B3}$$

Inserting this expression as a factor in the right side of Equation (B1) and eliminating m via Equation (B2), we obtain the following formula for the collapsing pressure:

$$p_{ultimate} = n_8 \sigma_y (t/a)^2 \tag{B4}$$

where

$$n_8 = \frac{12 - (1.3)(a/b)}{\left[\sqrt{3 + (a/b)^2} - (a/b)\right]^2} \tag{B5}$$

This equation is plotted in Figure 22. It is found that the resulting graph can be represented very well by the following second-degree parabola:

$$n_8 = 4 + 3.2\frac{a}{b} + 3.5\left(\frac{a}{b}\right)^2 \tag{B6}$$

Since this expression is much simpler, it will be used instead of (B5). Its substitution into Equation (B4) leads to Equation (27).

## REFERENCES


1. "Test Methods and Procedures for Microelectronics." MIL-STD-883-A, Rome Air Development Center (AFSC), Griffiss Air Force Base, New York, 15 November 1974.

2. Libove, C.: "Rectangular Flat-Pack Lids Under External Pressure." Final Report (Volume II) on Advanced Reliability and Maintainability Studies under Contract No. F30602-71-C-0312 with the Rome Air Development Center, Griffiss Air Force Base, New York. Syracuse University, Department of Industrial Engineering and Operations Research, Technical Report No. 74-2, September 1974. (Re-issued as RADC-TR-76-118, May 1976), (A025625).

3. Libove, C.: "Rectangular Flat-Pack Lids under External Pressure: Formulas for Screening and Design." 13th Annual Proceedings, Reliability Physics 1975, Las Vegas, Nevada, April 1-3, 1975, pp. 38-47. Publication No. 75CH0931-6 PHY, Institute of Electrical and Electronic Engineers, 345 East 47th Street, New York, New York 10017.

4. Timoshenko, S.; and Woinowsky-Krieger, S.: "Theory of Plates and Shells." McGraw-Hill Book Company, Inc., N.Y., 1959.

5. Kornishin, M.S.; and Isanbayeva, F.S.: "Flexible Plates and Panels." Report FTD-HC-23-441-69, Air Force Systems Command , Foreign Technology Division, January 21, 1971, AD 722 302. (Translation of Russian book Gibkiye Plastiny i Paneli, 1968).

6. Aalami, B.; and Williams, D.G.: "Thin Plate Design for Transverse Loading." John Wiley & Sons, N.Y., 1975.

7. Lin, T.H.; Lin, S.R.; and Mazelsky, B.: "Elastoplastic Bending of Rectangular Plates." Journal of Applied Mechanics, Dec. 1972, pp. 978-982.

8. "Properties of AlSiMag Brand Ceramics." Bulletin No. 757, Technical Ceramic Products Division, 3M Company, Saint Paul, Minnesota.

9. Jones, L.L.; and Wood, R.H.: "Yield-Line Analysis of Slabs." American Elsevier Publishing Co., Inc., N.Y., 1967.

10. Fox, E.N.: "Limit analysis for plates: the exact solution for a clamped square plate of isotropic homogeneous material obeying the square yield criterion and loaded by uniform pressure." Philosophical Transactions of the Royal Society of London; A. Mathematical and Physical Sciences, vol. 277, no. 1265, pp. 121-155, 29 August 1974.

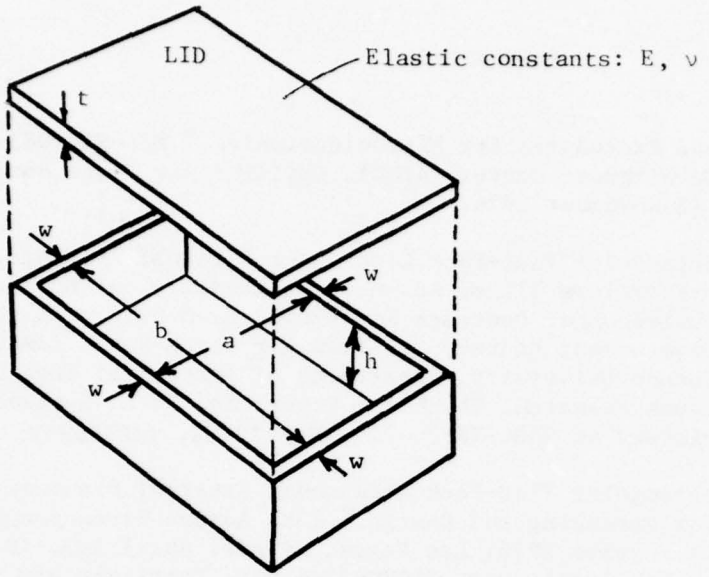


Figure 1.- Package configuration.

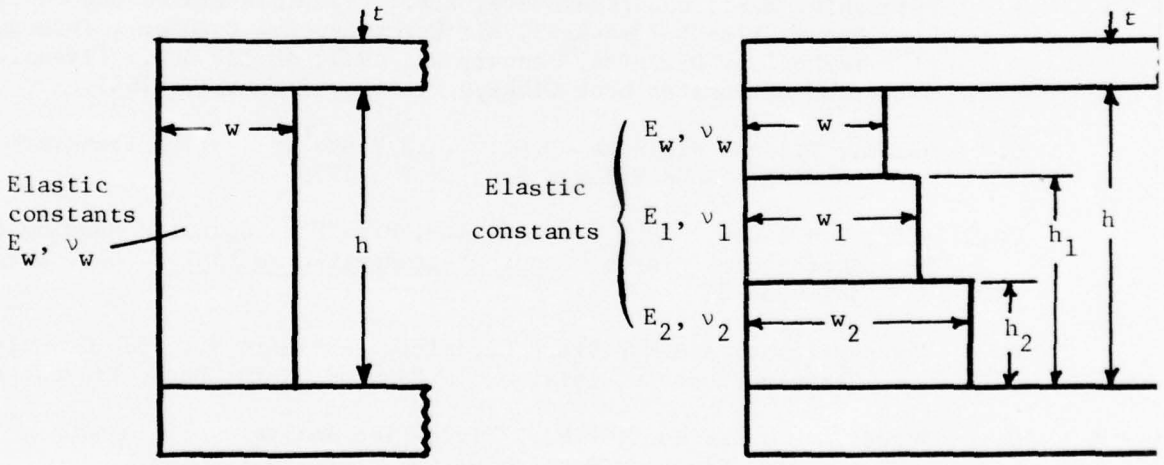


(a) Uniform wall

(b) Stepped wall

Figure 2.- Wall configurations.

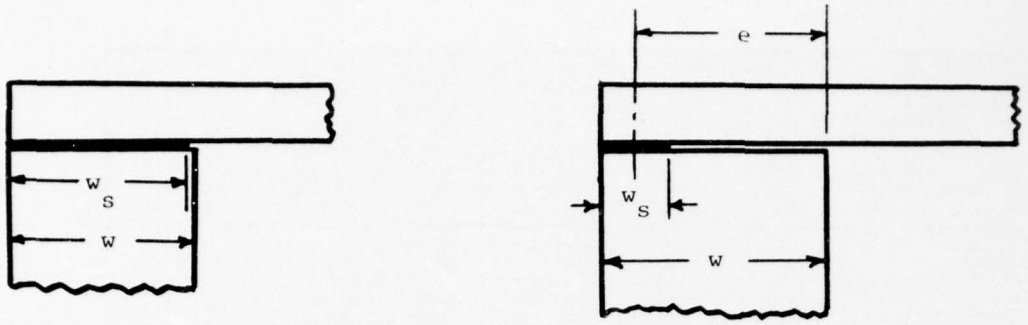


(a) Wide seal ($w_s \simeq w$)

(b) Narrow seal ($w_s << w$)

Figure 3.- Lid-to-wall seal geometries.

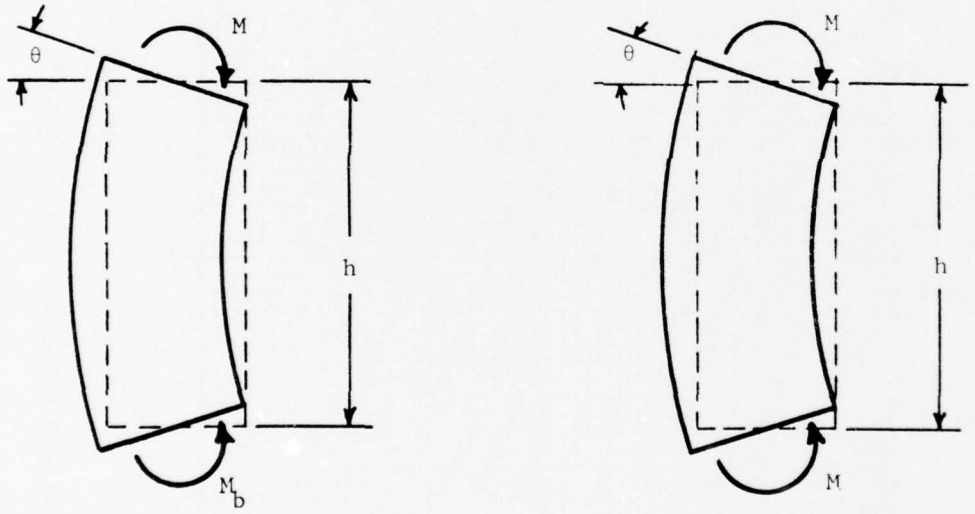


(a) Unequal moments at top and bottom of wall.

(b) Equal moments at top and bottom of wall.

Figure 4.- Wall flexure due to bending moments applied at top and bottom by lid and base.

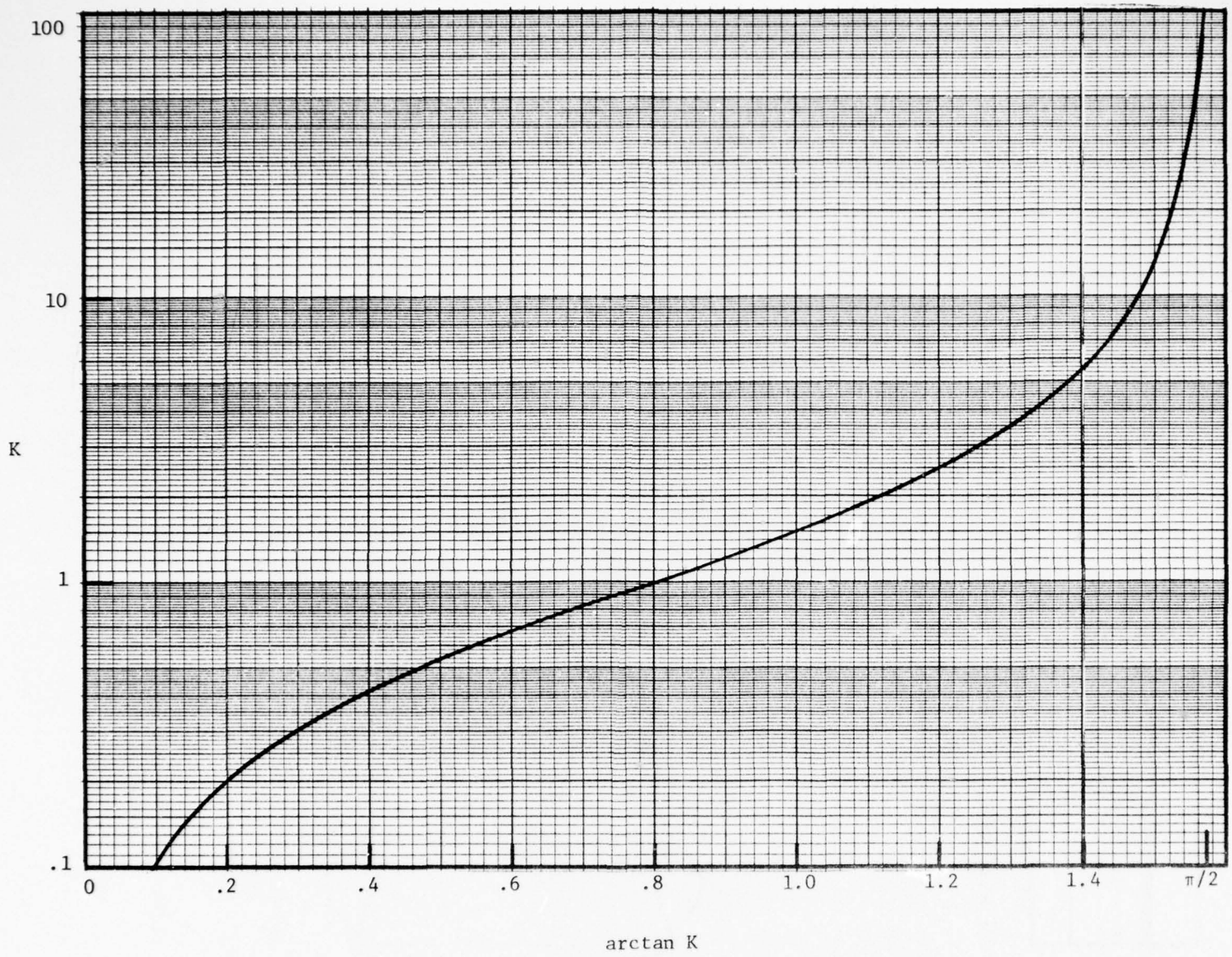


Figure 5.- Relationship between K and arctan K.

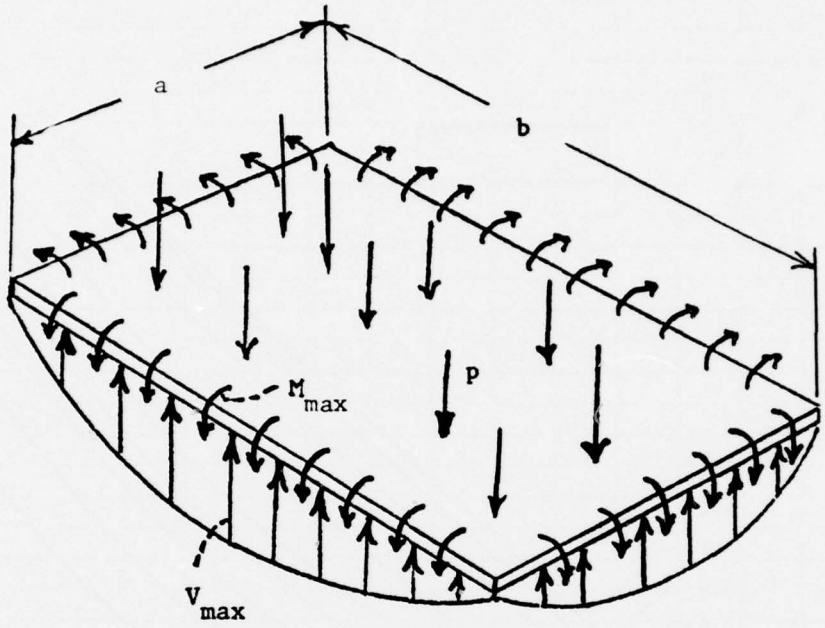


Figure 6.- Reactions on a uniformly loaded rectangular plate with edges elastically restrained against rotation.

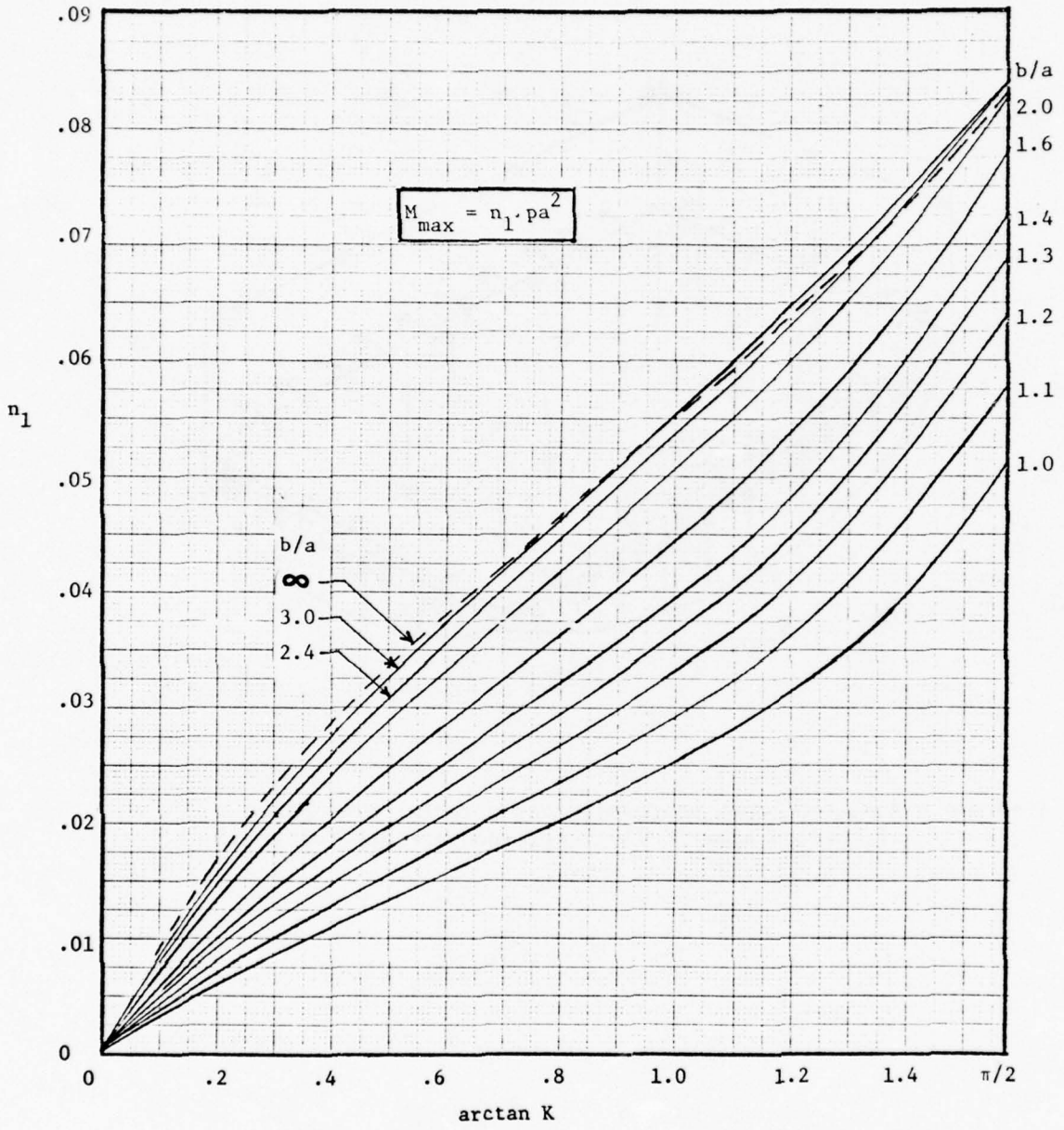


Figure 7.- Bending moment intensity at the middle of the long side for a uniformly loaded rectangular plate with edges elastically restrained against rotation.

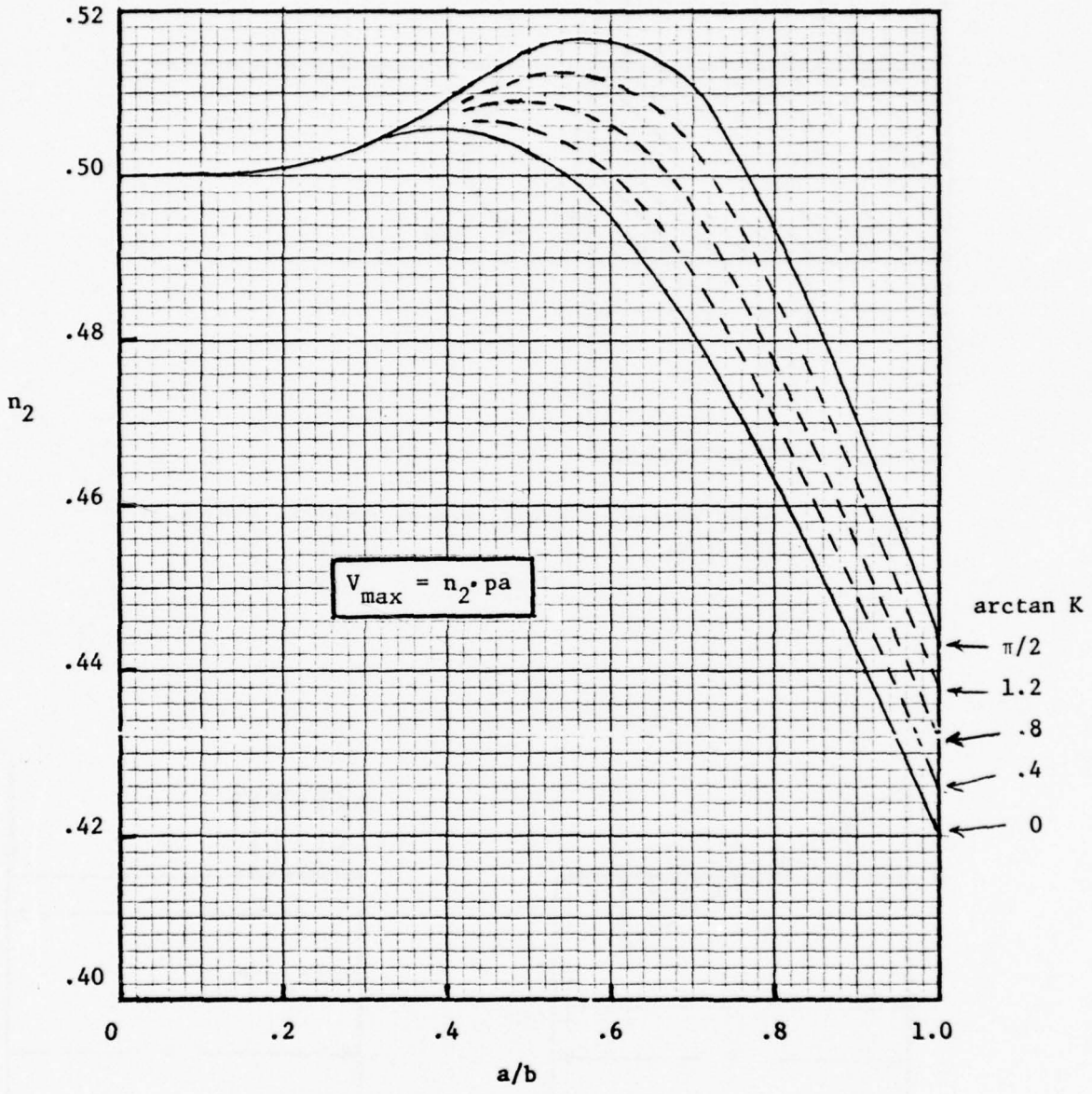


Figure 8.- Intensity of vertical reaction at the middle of the long side for a uniformly loaded rectangular plate with edges elastically restrained against rotation. ($\nu = 0.3$)

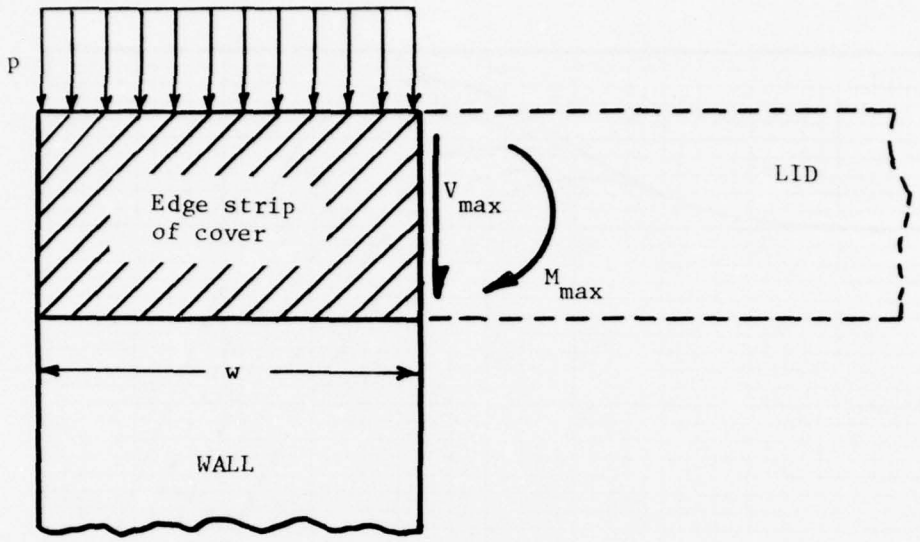


Figure 9.- Forces acting on edge strip of cover at middle of long side.

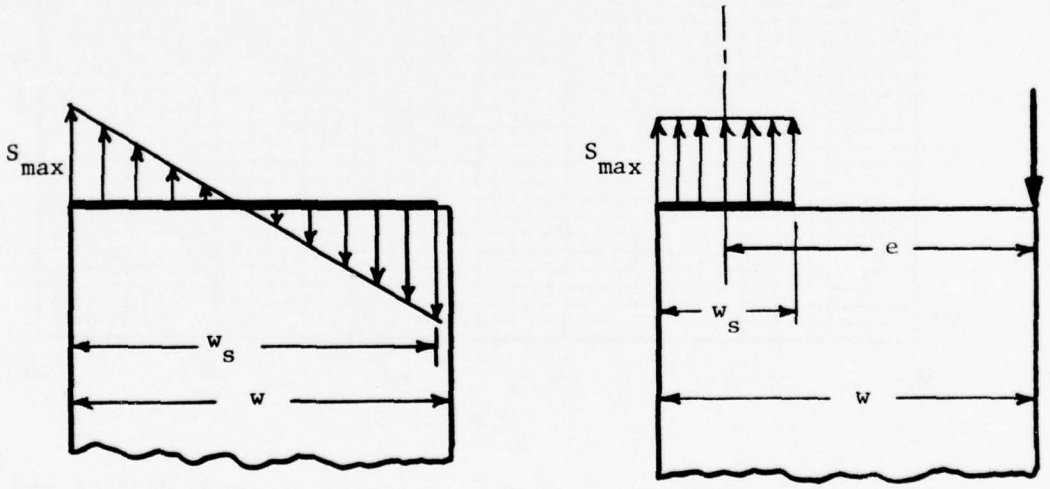


(a) Wide seal ($w_s \approx w$).

(b) Narrow seal ($w_s << w$)

Figure 10.- Stress distributions assumed across top of wall at middle of long side.

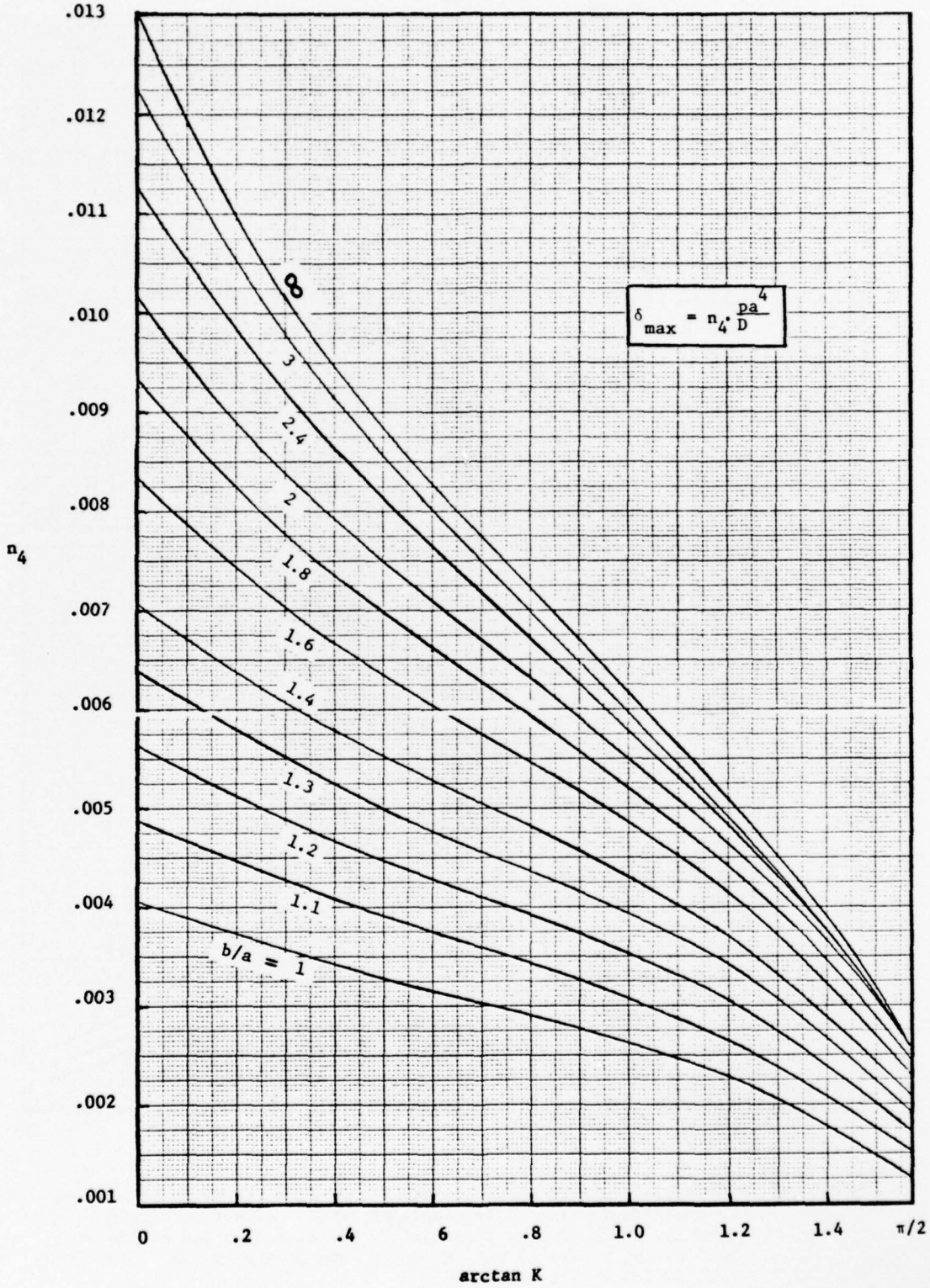


Figure 11.- Center deflection of a uniformly loaded rectangular plate with edges elastically restrained against rotation (small-deflection theory).

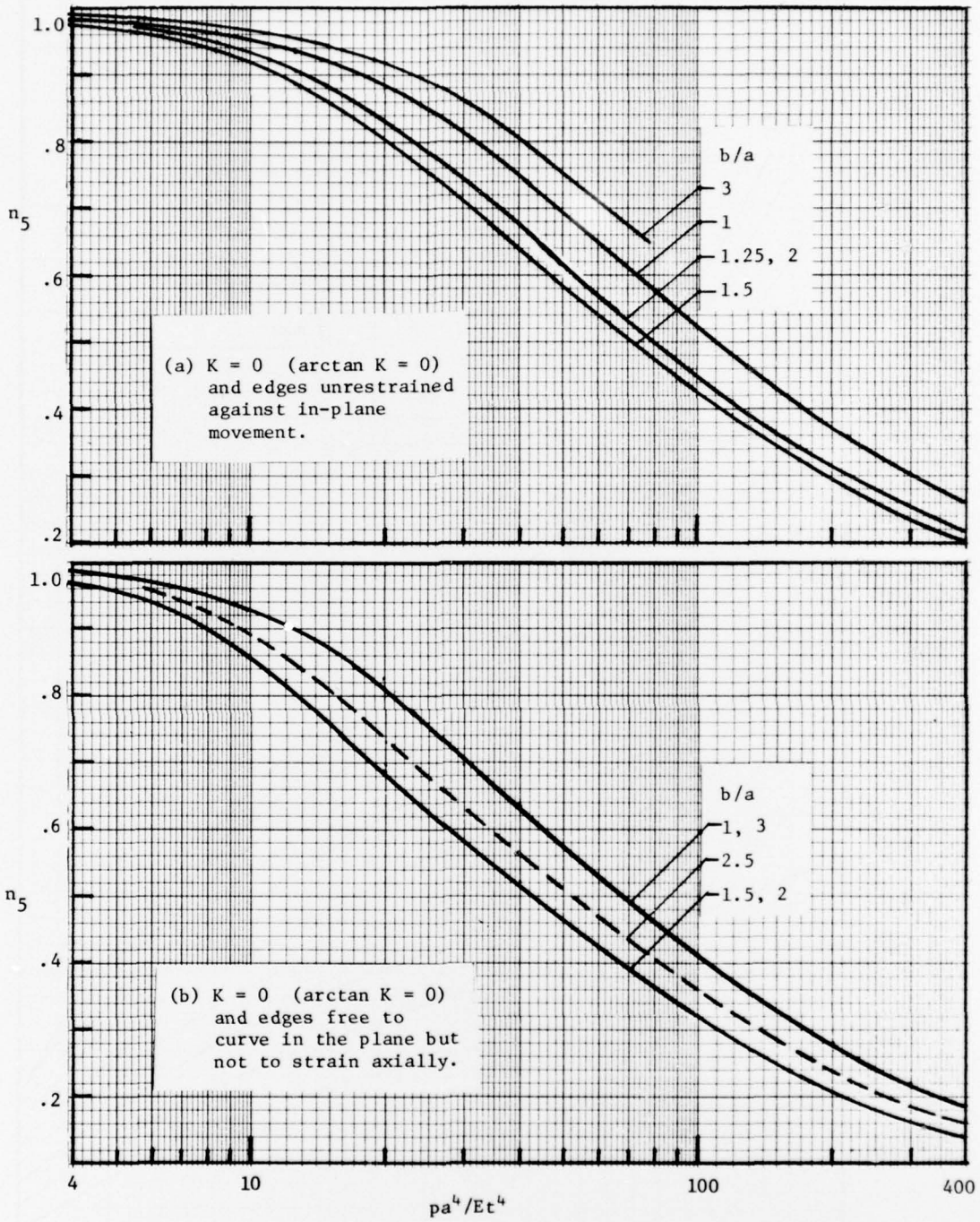


Figure 12.- Correction factors based on large-deflection theory to be applied to small-deflection theory value of center deflection of lid ($\nu$=0.3). Data adapted from: (a) P. 181 of Ref. 5 and p. 150 of Ref. 6. (b) P. 152 of Ref. 6. (c) P. 190 of Ref. 5 and p. 154 of Ref. 6. (c) P. 156 of Ref. 6.

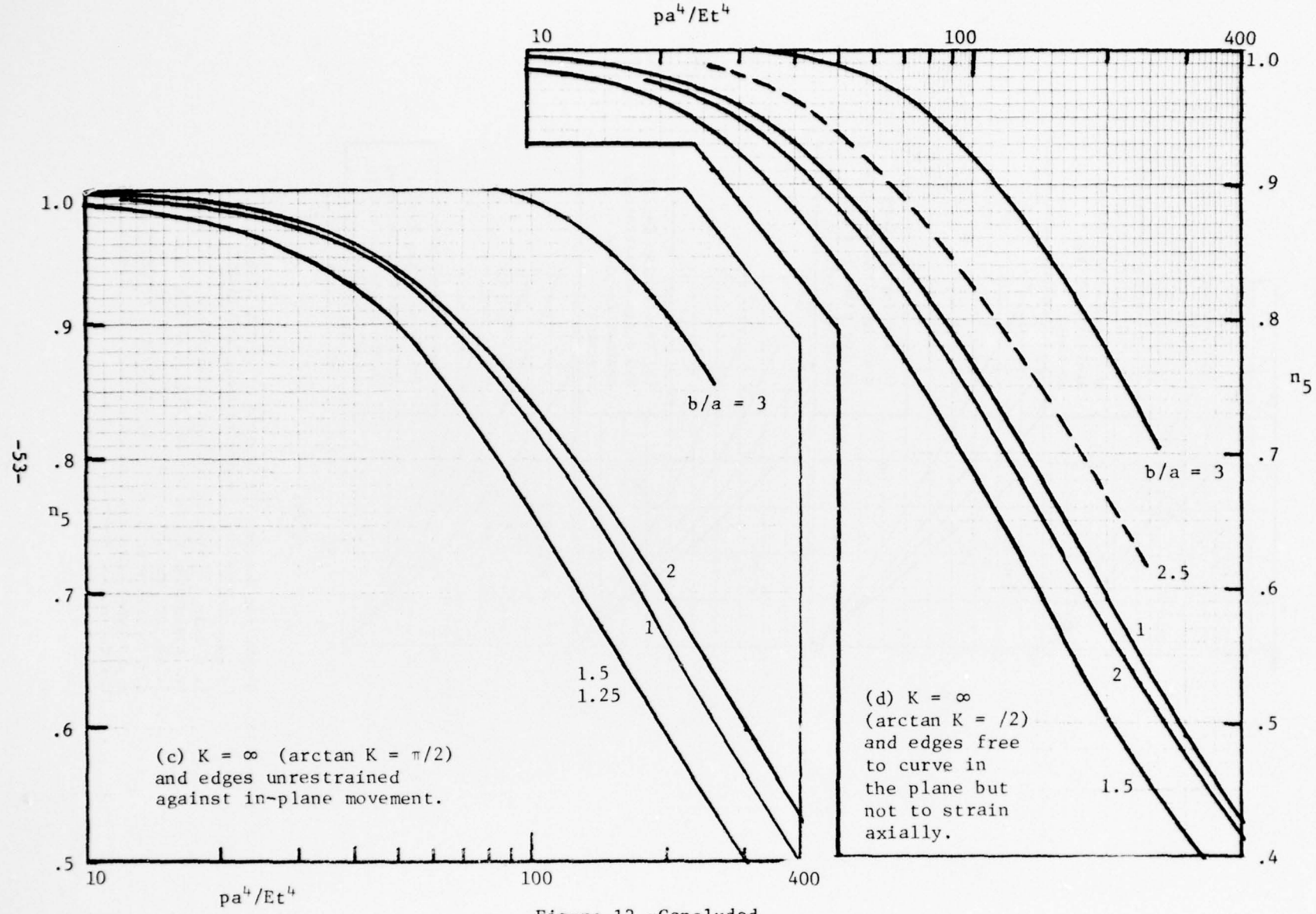


Figure 12.-Concluded.

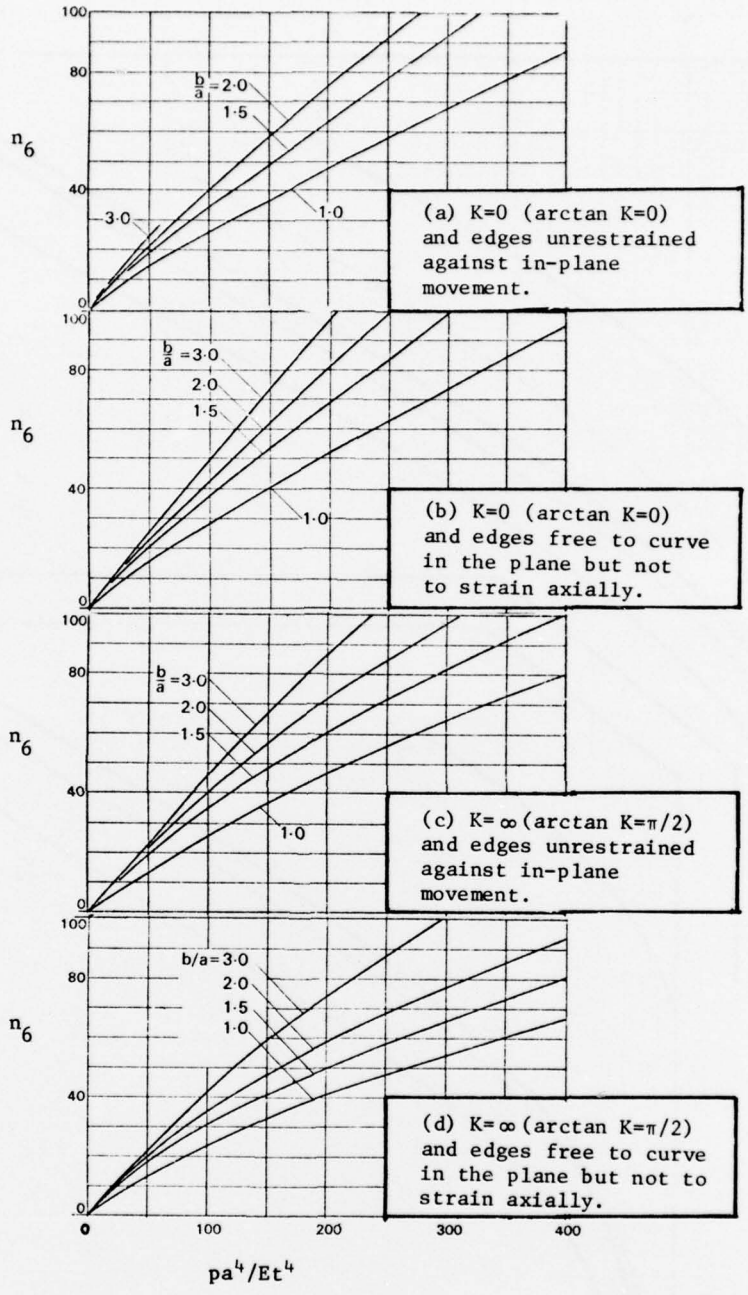


Figure 13.- Graphs for determining maximum effective stress $\sigma_{e\ max}$ in uniformly loaded rectangular plates ($\nu$ = 0.3). Source of curves: Reference 6, (a) top graphs on p. 50, (b) middle graphs on p. 48, (c) middle graphs on p. 50, and (d) middle graphs on p. 49. (By permission of copyright owner, Granada Publishing Ltd., St. Albans, Hertfordshire, England)

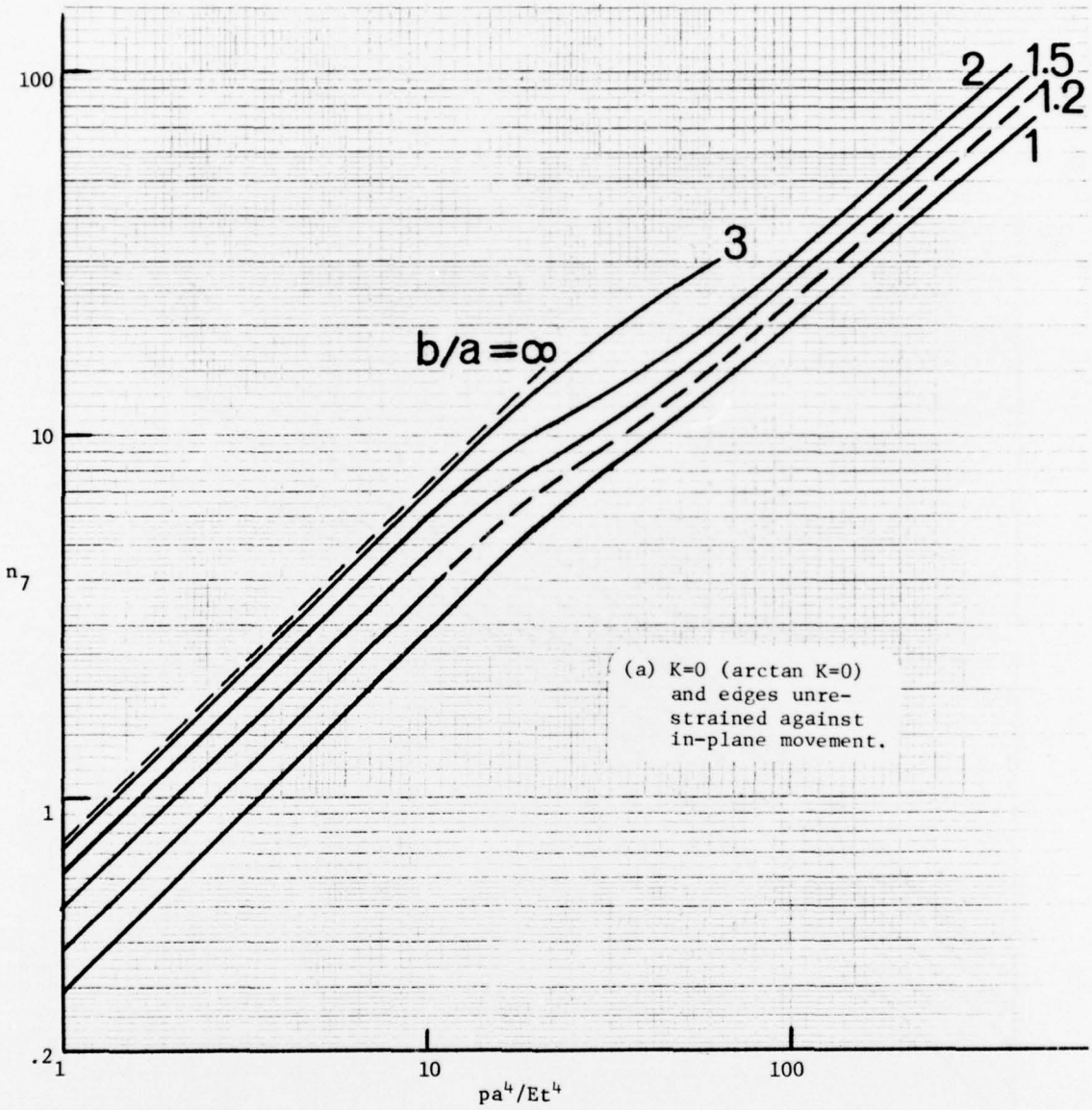


Figure 14.- Graphs for determining the maximum tensile stress $\sigma_{max}$ in uniformly loaded rectangular plates. Curves adapted from the following parts of Reference 6: (a) top graphs on p. 50, (b) middle graphs on p. 51, (c) middle graphs on p. 50, and (d) middle graphs on p. 52.

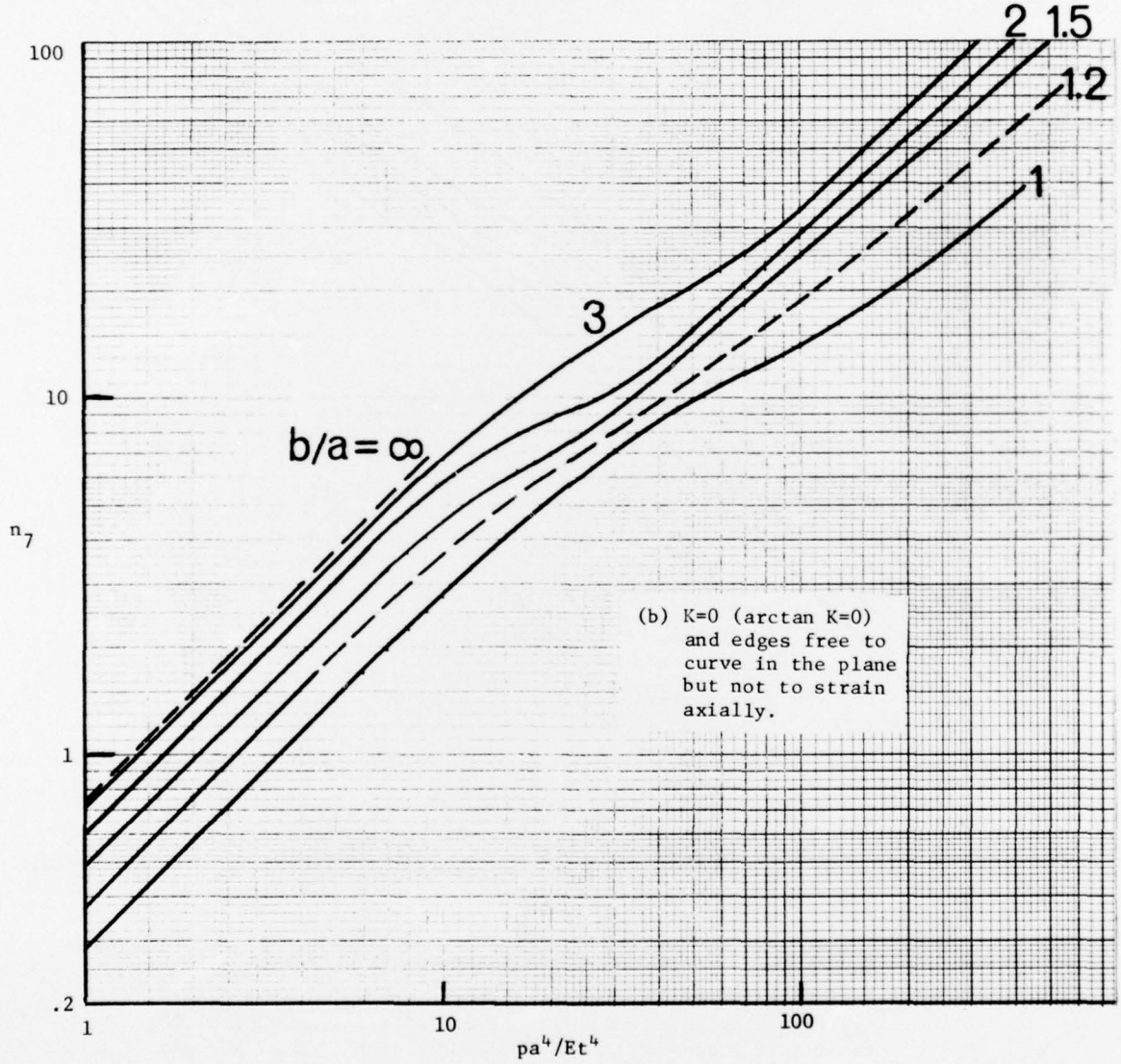


Figure 14.- Continued.

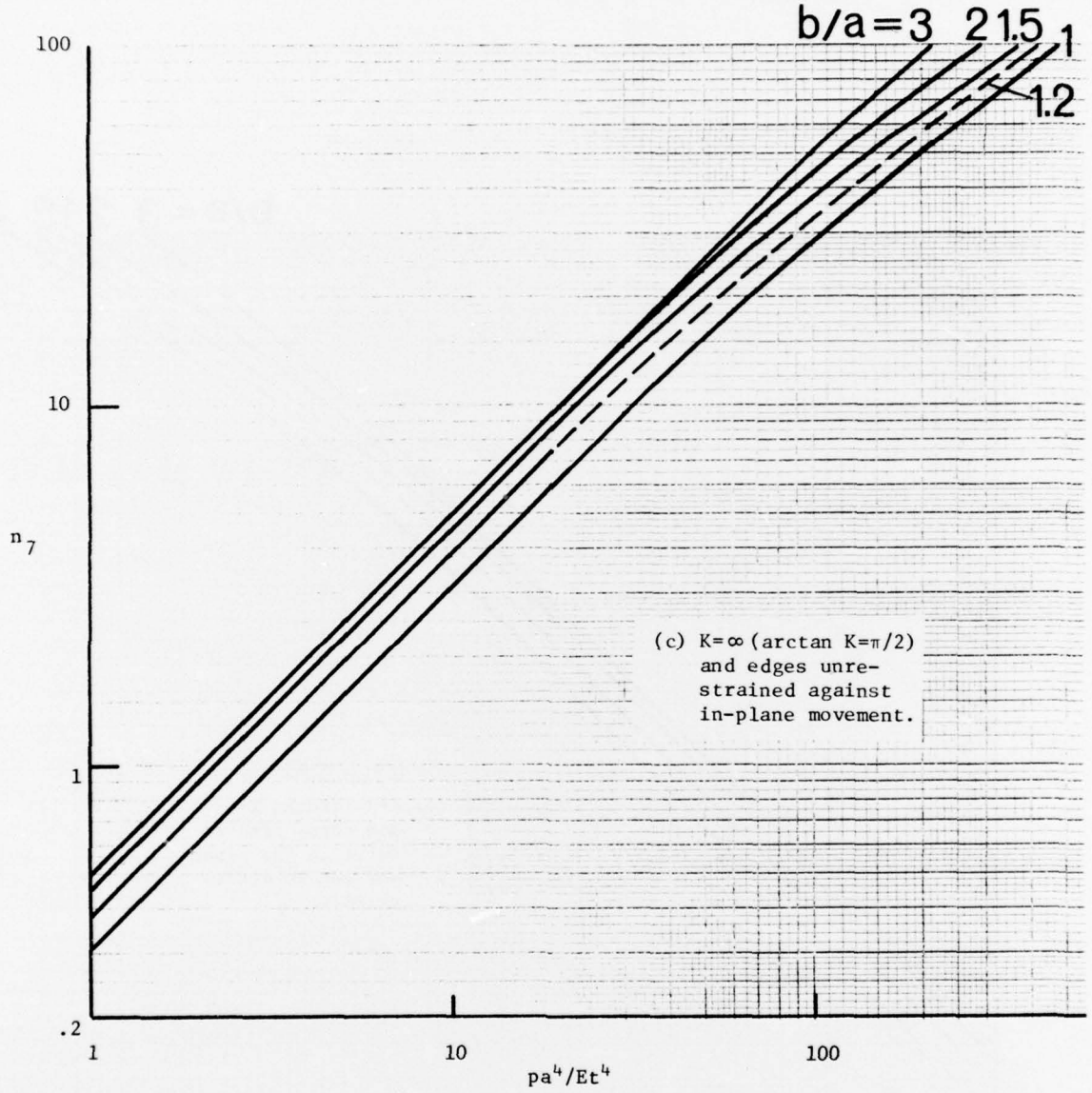


Figure 14.- Continued.

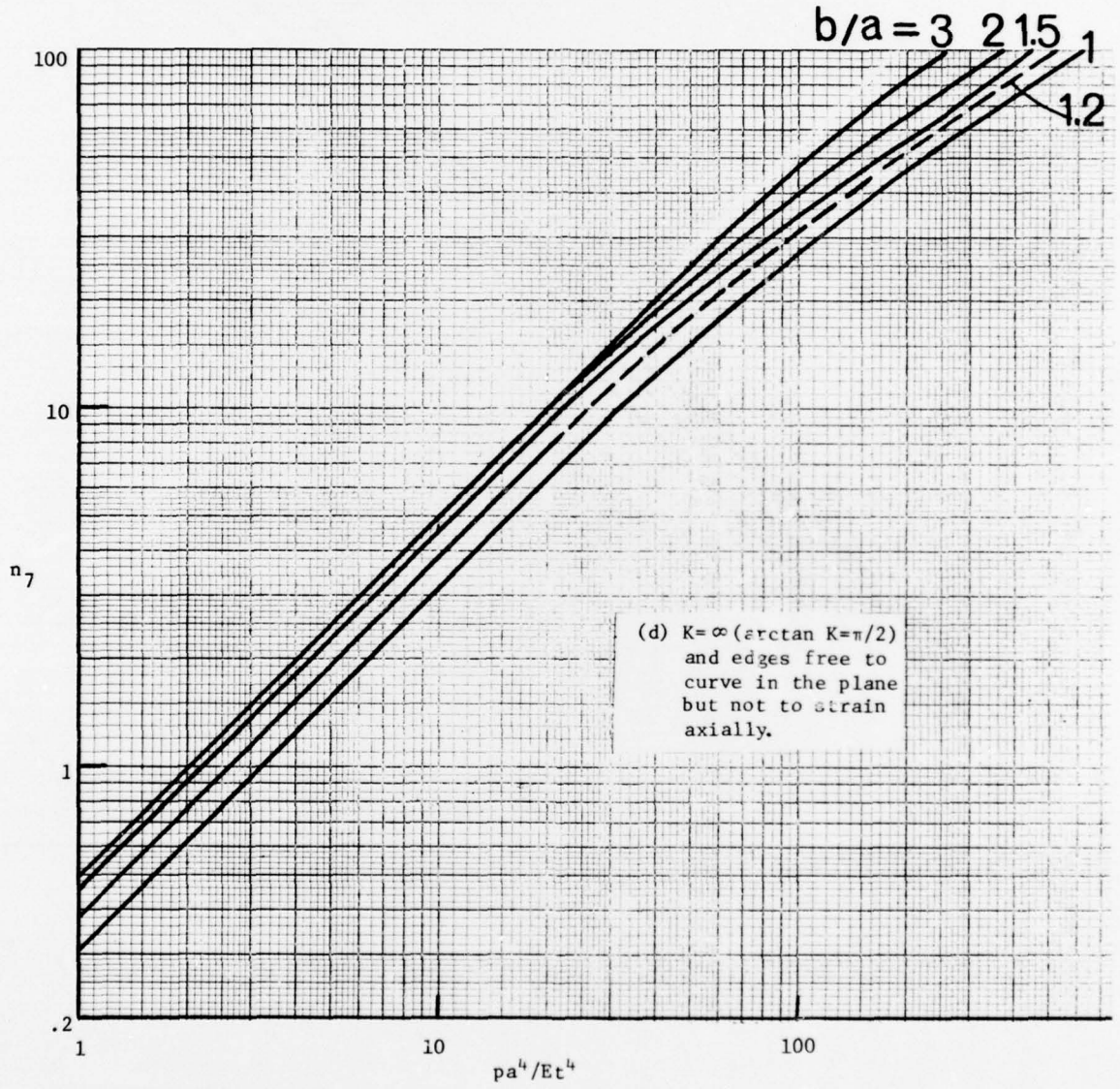


Figure 14.- Concluded.

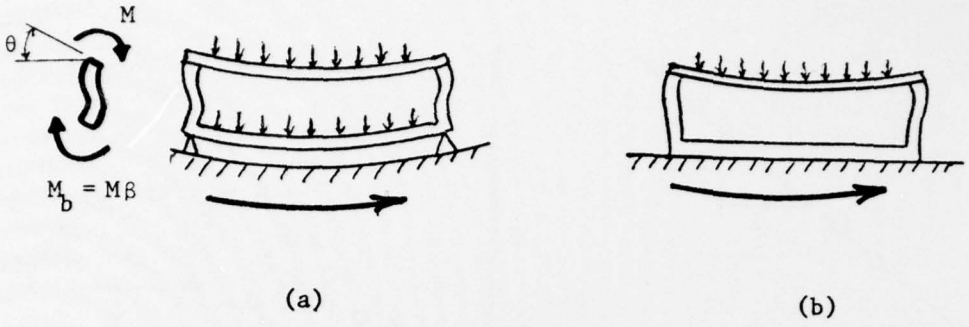


**Figure** 15.- Two possible kinds of lid-wall-base interaction for a package in a centrifuge.

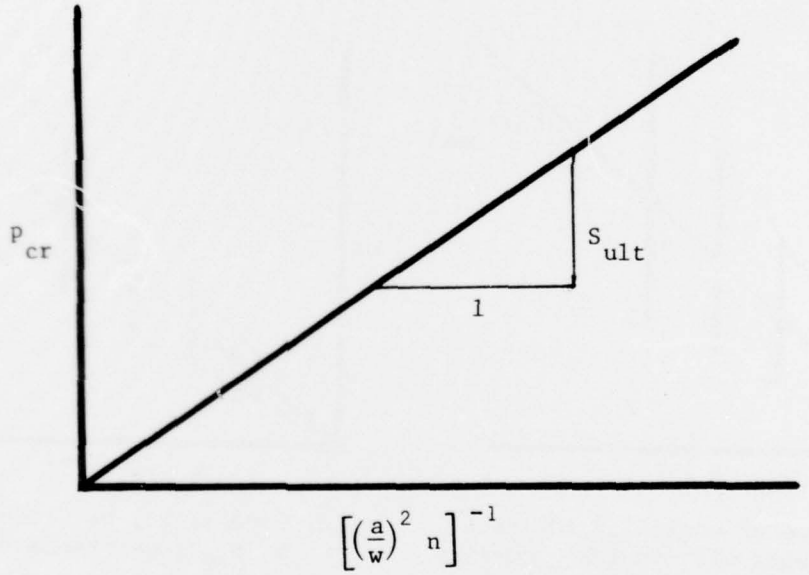


Figure 16.- Relationship implied by Eq. (37) between the pressure $p_{cr}$ causing loss of hermeticity and the package parameter $[(a/w)^2 n]^{-1}$.

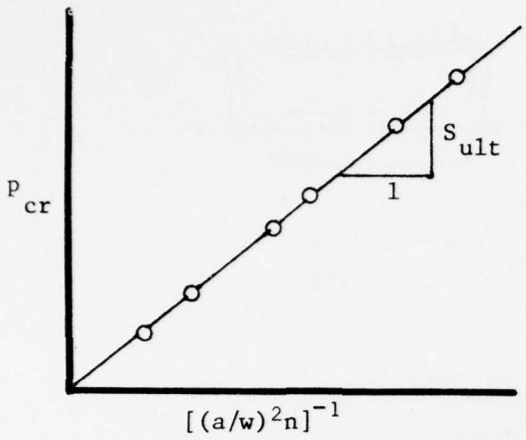


(a) Uniform quality seals.

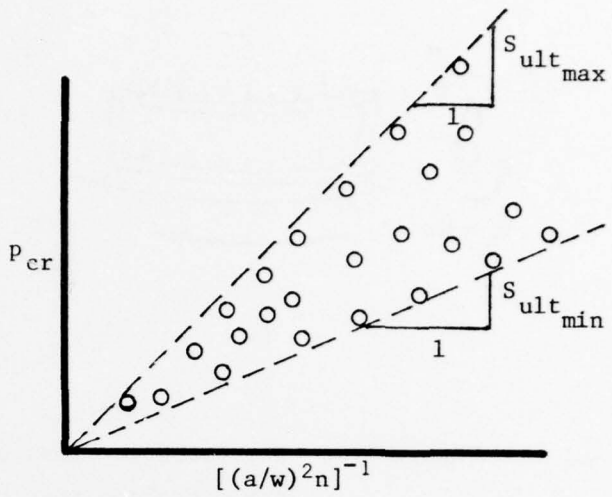


(b) Variable quality seals.

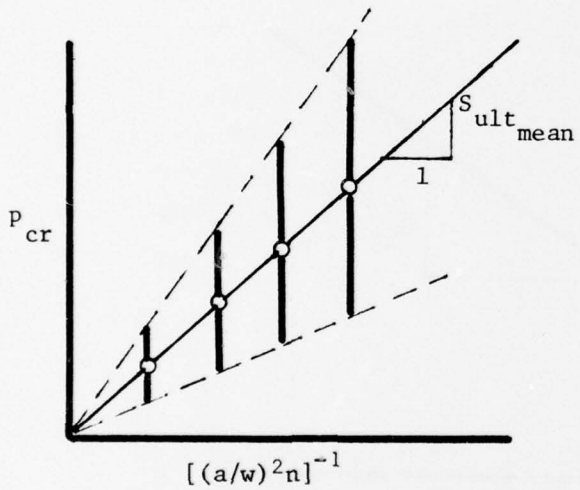


(c) Groups of nominally identical packages with variable quality seals; mean $p_{cr}$ (circle) and range of $p_{cr}$ plotted.

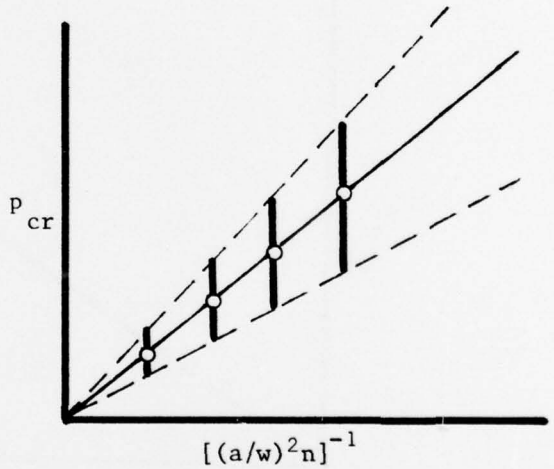


(d) Same as (c) but reduced range of $p_{cr}$ (one standard deviation above and below mean) plotted.

Figure 17.- Hypothetical satisfactory correlations between test data and theory (Eq. (37)).

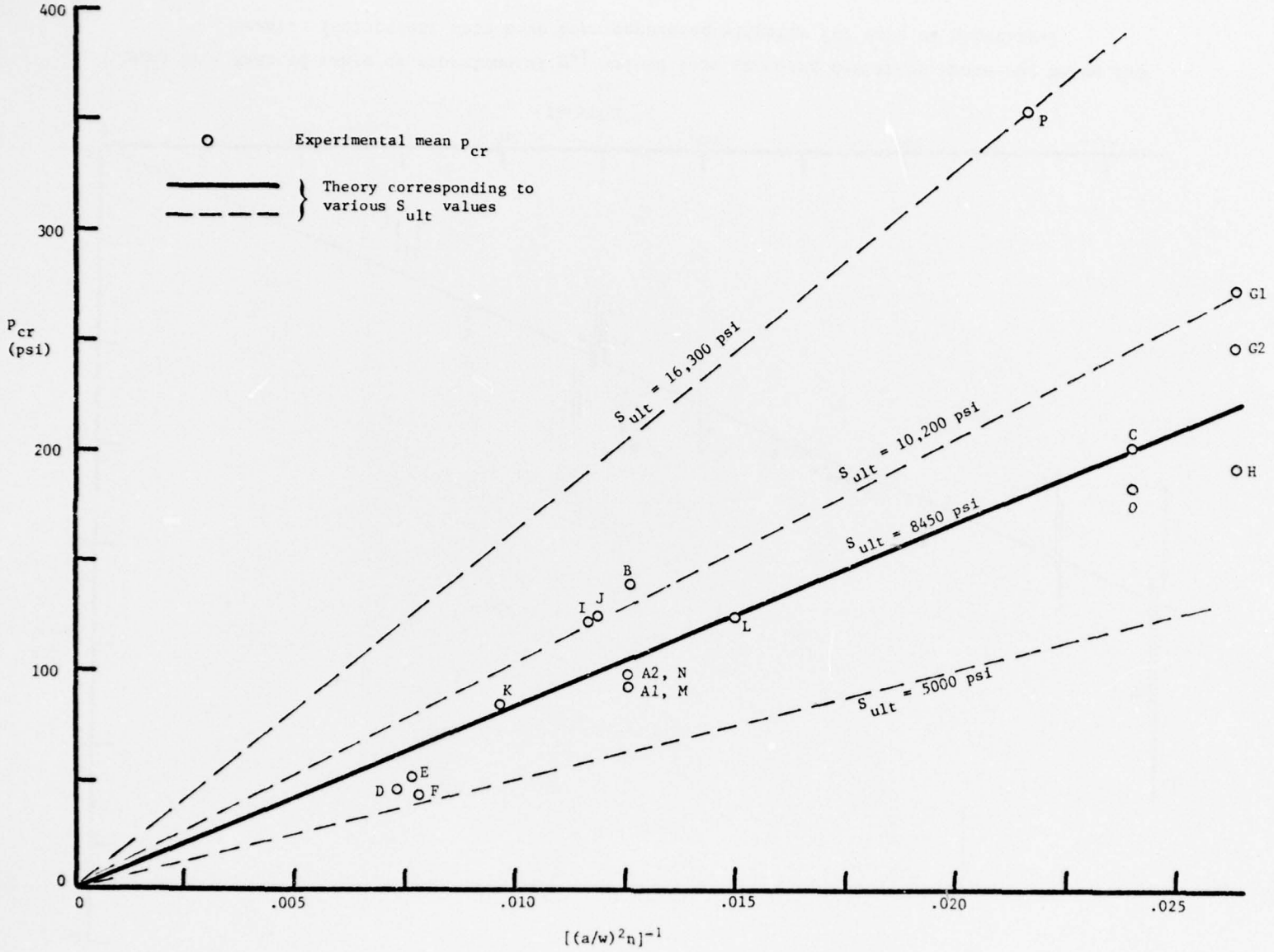


Figure 18.- Mean experimental values of $P_{cr}$ compared with theory.

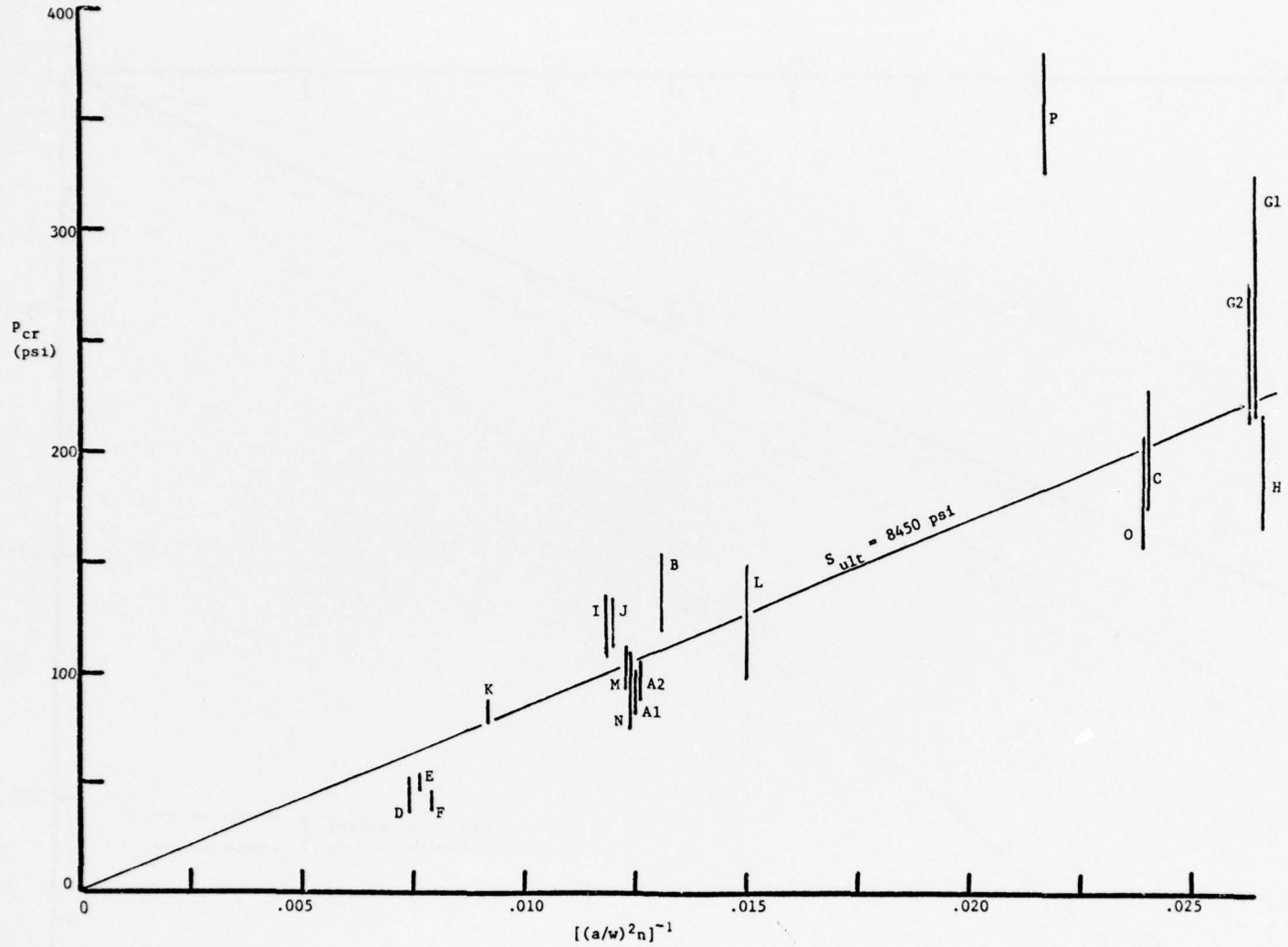


Figure 19.- Reduced range of experimental $p_{cr}$ values (one standard deviation above and below the mean). (Coincident data have been separated slightly for ease of plotting.)

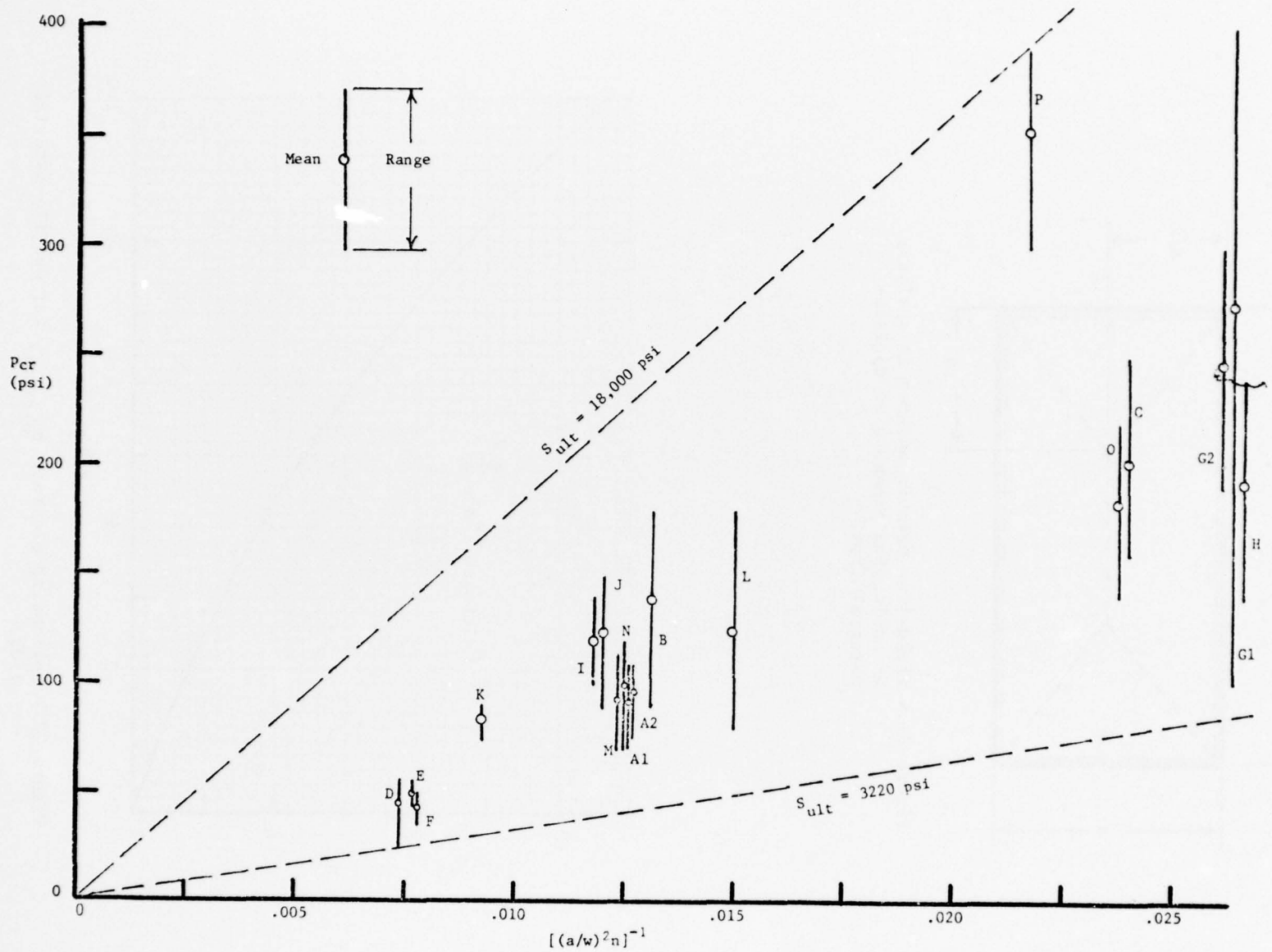


Figure 20.- Full range of experimental $p_{cr}$ values. (Coincident data have been separated slightly for ease of plotting.)

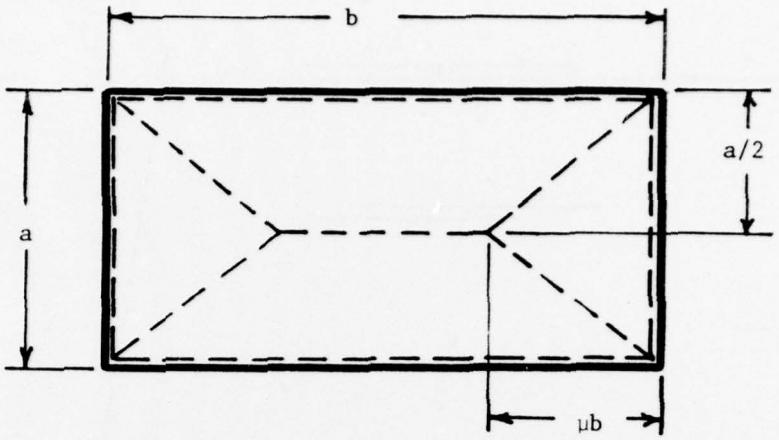


Figure 21.- Yield-line pattern assumed in analysis of collapsing pressure of ductile-material lids.

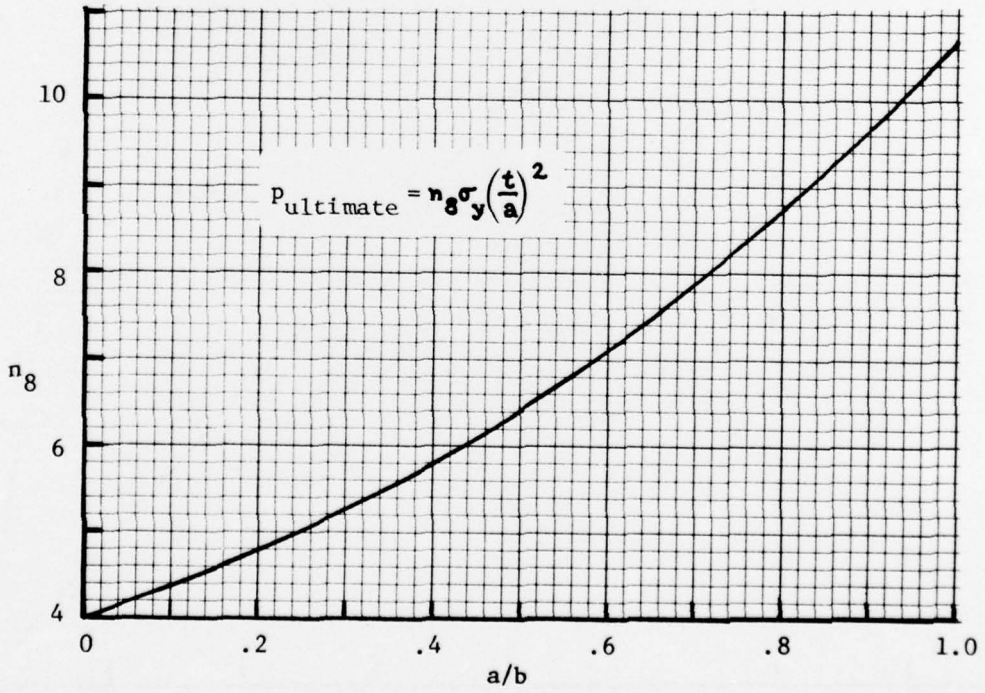


Figure 22.- Collapsing pressure $p_{ultimate}$ for ductile-material lids.

# *MISSION*
# *of*
# *Rome Air Development Center*

*RADC plans and conducts research, exploratory and advanced development programs in command, control, and communications ($C^3$) activities, and in the $C^3$ areas of information sciences and intelligence. The principal technical mission areas are communications, electromagnetic guidance and control, surveillance of ground and aerospace objects, intelligence data collection and handling, information system technology, ionospheric propagation, solid state sciences, microwave physics and electronic reliability, maintainability and compatibility.*